AD-A181 451 EXPERIMENTAL STUDIES OF JOINT FLEXIBILITY FOR PUMA 560 ROBOT(U) NAVAL POSTGRADUATE SCHOOL MONTEREY CA D K GONYIER MAR 87 1/1

UNCLASSIFIED F/G 13/9 NL

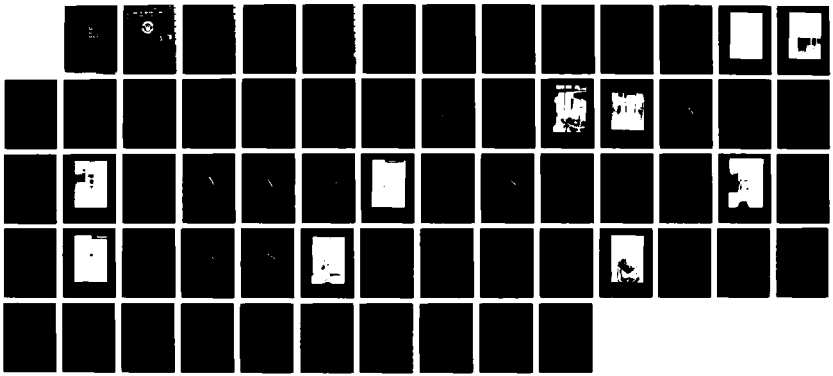

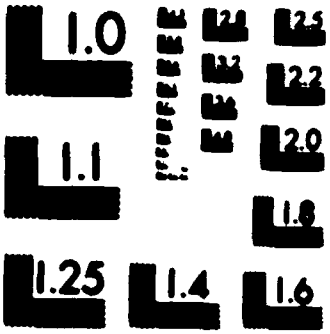

MICROCOPY RESOLUTION TEST CHART
NATIONAL BUREAU OF STANDARDS 1963 A

DTIC FILE COPY

AD-A181 451

NAVAL POSTGRADUATE SCHOOL
Monterey, California

DTIC
ELECTE
JUN 1 9 1987
S D
E

THESIS

EXPERIMENTAL STUDIES OF JOINT FLEXIBILITY FOR PUMA 560 ROBOT

by

Dennis K. Gonyier

March 1987

Thesis Advisor: L. W. Chang

Approved for public release; distribution is unlimited.

87 132

SECURITY CLASSIFICATION OF THIS PAGE

AD-A181 451

REPORT DOCUMENTATION PAGE

1a REPORT SECURITY CLASSIFICATION UNCLASSIFIED	1b RESTRICTIVE MARKINGS
2a SECURITY CLASSIFICATION AUTHORITY	3 DISTRIBUTION/AVAILABILITY OF REPORT Approved for public release; distribution is unlimited.
2b DECLASSIFICATION/DOWNGRADING SCHEDULE	
4 PERFORMING ORGANIZATION REPORT NUMBER(S)	5 MONITORING ORGANIZATION REPORT NUMBER(S)
6a NAME OF PERFORMING ORGANIZATION Naval Postgraduate School 6b OFFICE SYMBOL (If applicable) 69	7a NAME OF MONITORING ORGANIZATION Naval Postgraduate School
6c ADDRESS (City, State, and ZIP Code) Monterey, California 93943-5000	7b ADDRESS (City, State, and ZIP Code) MOnterey, California 93943-5000
8a NAME OF FUNDING/SPONSORING ORGANIZATION Research Council 8b OFFICE SYMBOL (If applicable)	9 PROCUREMENT INSTRUMENT IDENTIFICATION NUMBER
8c ADDRESS (City, State, and ZIP Code) Naval Postgraduate School Monterey, California 93943	10 SOURCE OF FUNDING NUMBERS PROGRAM ELEMENT NO / PROJECT NO / TASK NO / WORK UNIT ACCESSION NO

11 TITLE (Include Security Classification)

EXPERIMENTAL STUDIES OF JOINT FLEXIBILITY FOR PUMA 560 ROBOT

12 PERSONAL AUTHOR(S)

Gonyier, Dennis K.

13a TYPE OF REPORT	13b TIME COVERED	14 DATE OF REPORT (Year, Month, Day)	15 PAGE COUNT
Master's Thesis	FROM ____ TO ____	1987 March	63

16 SUPPLEMENTARY NOTATION

17 COSATI CODES			18 SUBJECT TERMS (Continue on reverse if necessary and identify by block number)
FIELD	GROUP	SUB-GROUP	Manipulator flexibilities, robotics.

19 ABSTRACT (Continue on reverse if necessary and identify by block number)

This paper investigates flexibility of the PUMA 560 industrial robot arm. The purpose is accomplished by measurement of the flexural stiffness of the key joints in the system. The joint flexibilities are linear in nature and a torsional spring constant 'k', is determined for each joint. This data is necessary for the inclusion of flexibility effects into the equations of motion.

20 DISTRIBUTION/AVAILABILITY OF ABSTRACT ☒ UNCLASSIFIED/UNLIMITED ☐ SAME AS RPT ☐ DTIC USERS	21 ABSTRACT SECURITY CLASSIFICATION UNCLASSIFIED
22a NAME OF RESPONSIBLE INDIVIDUAL Professor Chang, Code 69Ck	22b TELEPHONE (Include Area Code) (408) 646-2632 / 22c OFFICE SYMBOL 69Ck

DD FORM 1473, 84 MAR 83 APR edition may be used until exhausted. All other editions are obsolete

SECURITY CLASSIFICATION OF THIS PAGE

Approved for public release; distribution is unlimited.

Experimental Studies of Joint Flexibility For PUMA 560 Robot

by

Dennis Keith Gonyier
Lieutenant, United States Navy
B.S. Purdue University, 1979

Submitted in partial fulfillment of the requirements for the degree of

MASTER OF SCIENCE IN MECHANICAL ENGINEERING

from the

NAVAL POSTGRADUATE SCHOOL
March 1987

Author: _____
Dennis K. Gonyier

Approved by: _____
Liang-Wey Chang, Thesis Advisor

_____
Anthony J. Healey, Chairman
Department on Mechanical Engineering

_____
Gordon E. Schacher,
Dean of Science and Engineering

ABSTRACT

This paper investigates flexibility of the PUMA 560 industrial robot arm. The purpose is accomplished by measurement of the flexural stiffness of the key joints in the system. The joint flexibilities are linear in nature and a torsional spring constant 'k', is determined for each joint. This data is necessary for the inclusion of flexibility effects into the equations of motion.

Accession For
NTIS GRA&I ☒
DTIC TAB ☐
Unannounced ☐
Justification
By
Distribution/
Availability Codes
Dist | Avail and/or Special
A-1

QUALITY INSPECTED 1

TABLE OF CONTENTS

I. INTRODUCTION 7

A. FLEXIBLE MANIPULATOR USES 7

B. BACKGROUND 8

C. SYSTEM DESCRIPTION 9

D. SYSTEM LIMITATIONS 15

II. ERROR INDUCING FACTORS 16

III. FLEXIBILITY MEASUREMENTS 18

A. STATIC MEASUREMENTS 18

B. JOINT ONE RESULTS 18

C. JOINT TWO RESULTS 25

D. JOINT THREE RESULTS 28

E. JOINTS FOUR, FIVE AND SIX 33

F. DYNAMIC MEASUREMENT 46

IV. CONCLUSIONS 52

V. RECOMMENDATIONS 53

LIST OF REFERENCES 54

APPENDIX: EXPERIMENTAL DATA TABLES 55

INITIAL DISTRIBUTION LIST 61

LIST OF FIGURES

Figure 1. PUMA 560 Industrial Robot Arm 10
Figure 2. PUMA 560 Computer and I/O Equipement 11
Figure 3. Operating Envelope 12
Figure 4. Robot Arm Link Identification 14
Figure 5. Joint One Gear Train 19
Figure 6. Joint One Experiment (CCW) 21
Figure 7. Joint One Experiment (CW) 22
Figure 8. Joint One Data 23
Figure 9. Joint One Curve Fit 24
Figure 10. Joint Two Gear Train 25
Figure 11. Joint Two Experiment 26
Figure 12. Joint Two Data 29
Figure 13. Joint Two Curve Fit 30
Figure 14. Joint Three Gear Train 31
Figure 15. Joint Three Experiment 32
Figure 16. Joint Three Data 33
Figure 17. Joint Three Curve Fit 35
Figure 18. Wrist Articulation 36
Figure 19. Joint Four Experiment 38

Figure 20. Joint Four Data 39

Figure 21. Joint Four Curve Fit 40

Figure 22. Joint Five Experiment 41

Figure 23. Joint Five Data 43

Figure 24. Joint Five Curve Fit 44

Figure 25. Joint Six Experiment 45

Figure 26. Joint Six Data 47

Figure 27. Joint Six Curve Fit 48

Figure 28. Shoulder Link Drive Train 50

I. INTRODUCTION

A. FLEXIBLE MANIPULATOR USES

There is a potential in the Navy and the Department of Defense for the utilization of robot manipulators in a wide range of applications.

First, they could be used in applications that are performed in environments dangerous to men. These include under-water work, fire fighting, tank and void preservation and reactor spaces.

Second, many patrol and/or security functions could be performed by robot devices releasing the operator to a position of supervisory control over many units.

Third, robotic submersibles are being used now to explore areas of our under-sea environment that were out of economical range before their use. This will lead to a closer determination of the resources available in our oceans and their subsequent exploitation.

There is also a large potential for the use of robots in space. The weight limitations will demand manipulators to be "flexible" compared to the industrial machines currently available. The problems of control of these "flexible" arms will have to be studied prior to their implementation.

In addition, the robot manipulators currently installed in industry have the potential for increased productivity if their performance could be enhanced. The enhanced performance

demands the understanding of the flexibility effects and their integration into the control algorithm. (Theses),

B. BACKGROUND

The theroretical aspects of joint flexibilities, link parameter variations, gear eccentricity and gear-lash in the PUMA 560 robot were discussed by Ahamad.[Ref.1] He developed models for each of the effects and proposes compensation schemes based on PID control. The problem of measurment of link parameter variations was discussed and several references were given. The model for gear eccentricity showed that the effects produced very small inaccuracies. It was proposed that the gear eccentricity effects are relatively negligable compared to the other effects. The predicted effects of gear lash is modeled as lost motion. The effects of joint flexibility are postulated to add an angular error that is proportional to the joint torque load.

Good, Sweet and Strobel [Ref.2] discuss high performance robot motion controls and emphasize the importance of compensating the flexible effects. The joint flexibilities also contribute to the natural frequencies of the system and the modeling of the flexibilities is fundumental to the development of high performance robot controls.

The purpose of this thesis is to investigate the flexibility of the PUMA 560 industrial robot arm and to provide this information for the modeling of flexibility into the equations of motion. The

purpose is accomplished by measurement of the flexural stiffness of the key joints in the system.

C. SYSTEM DESCRIPTION

The PUMA 560 robot is an industrial robot system with six degree of freedom. It is comprised of a robot arm (Figure 1), a controller (Figure 2), software and peripherals. It is designed to manipulate a nominal end-effector load of 2.5kg with a positional repeatability of 0.1mm. It has a spherical work envelope of 0.92m (Figure 3). The maximum tool velocity is 1.0 m/s and the maximum tool acceleration is 1.0 g. The maximum static force at the tool is 58 N. [Ref.3]

The Puma 560 is controlled by a closed-loop control system. Incremental encoders and potentiometers at each drive motor provide the positional feedback for the control system. Each of the joint encoders provides a resolution of approximately .005 degree/bit. The repeatability feature of the robot system is attained when specific points are designated as precision points. This causes the system to remember specific joint angles with the end-effector and its load in position. The PUMA 560 robot can be programmed to move to successive precision points, or can be positioned using transformations. [Ref.4] When programmed using transformations (off-line) there is no mechanism to compensate for the effects of the load on the final position. A move from a known position to a specific coordinate may or may not result in the end-effector attaining the desired final position.

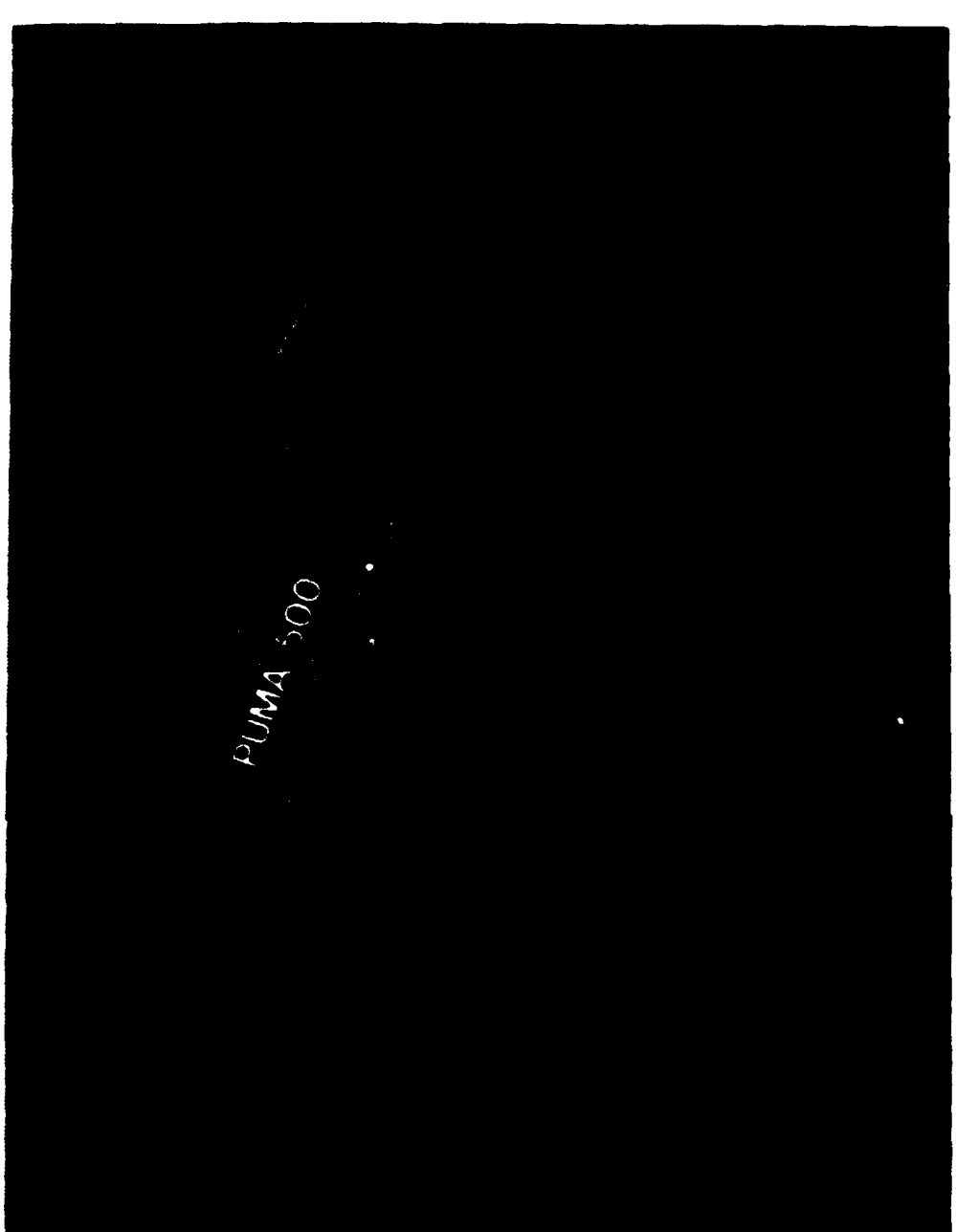

Figure 1. PUMA 560 Industrial Robot Arm

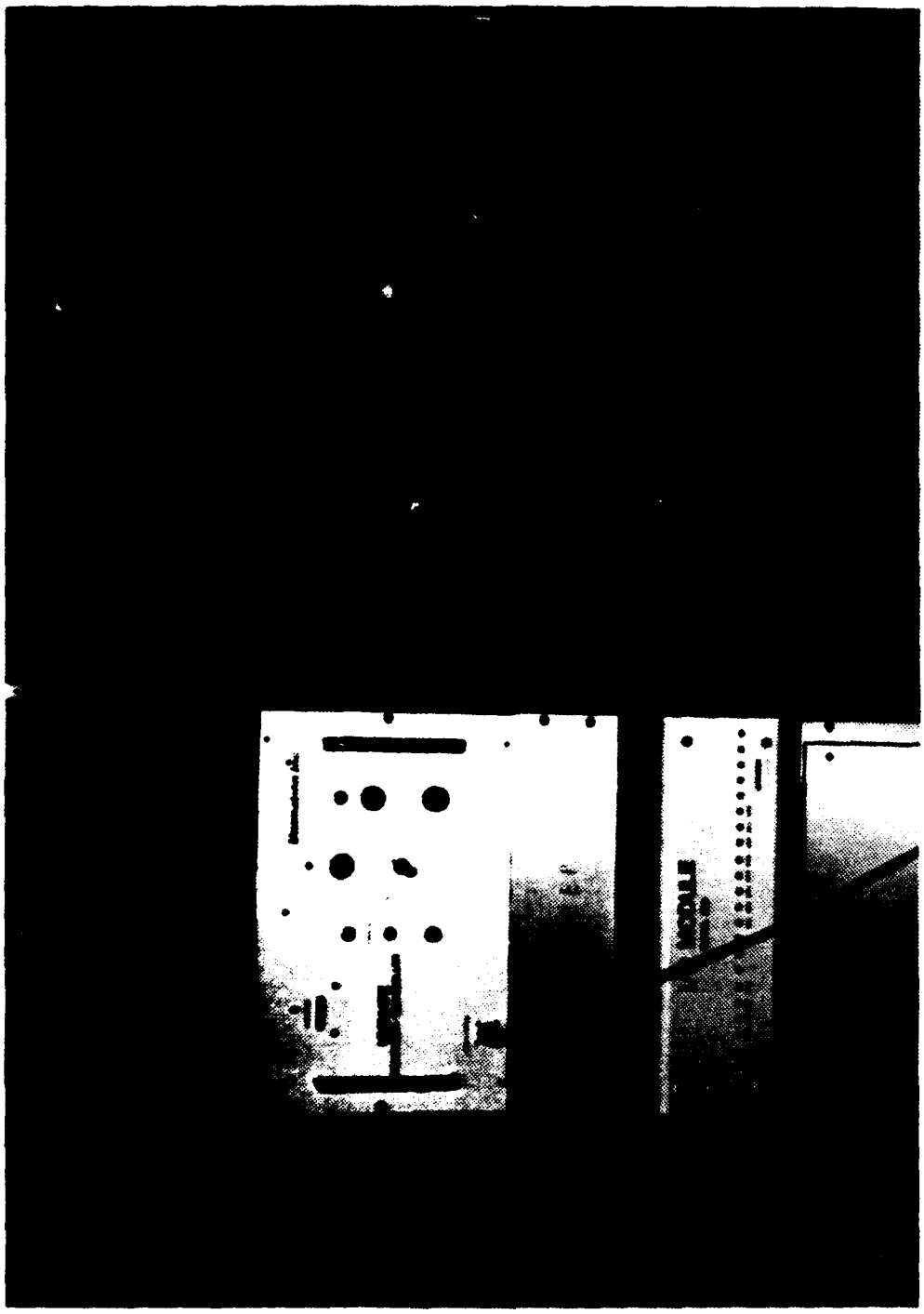

Figure 2. PUMA 560 Computer and I/O Equipement

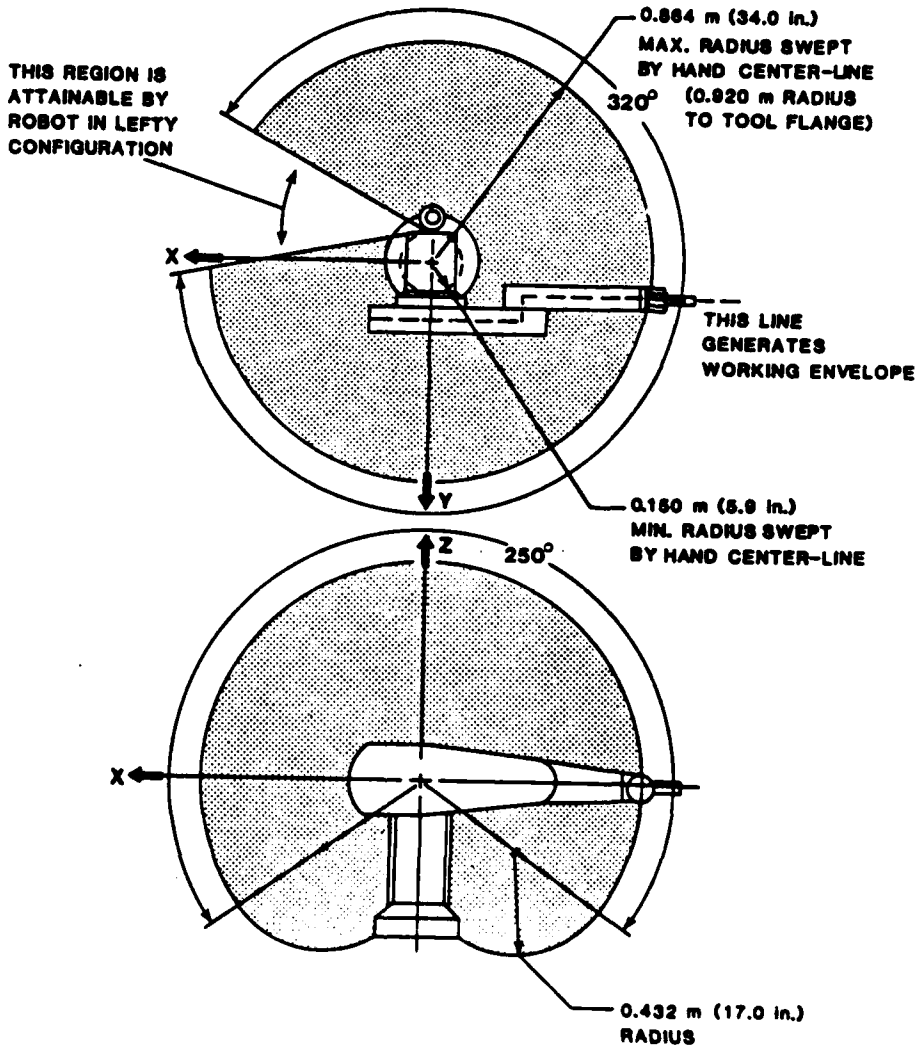

Figure 3. Operating Envelope [Ref. 3]

1. Robot Arm

The robot arm is the mechanical component of the system. It consists of the trunk, shoulder, upper arm, forearm, wrist and gripper (Figure 4). Each member of the assembly is driven by a permanent-magnet DC servomotor through its associated gear train. Each drive motor contains a direct driven incremental shaft encoder and a potentiometer driven through a 116 to 1 gear drive. Each time the system is powered, up the initializing routine uses the potentiometer to establish absolute position. During subsequent operation, the encoder is sampled every .88 millisecond for position and the velocity is calculated. This information is used for positional feedback in the control system.

Each joint drive is driven through at least two sets of precision gears. Several joints have pairs of flexible helical spring couplings included in their respective drive lines. The flexible couplings ensure a smooth transmission of motion while allowing for mechanical misallignment and relative movement between the frame mounted drive motors and various drive trains.

2. Controller

The controller contains the backplane computer, signal processing, power amplifiers and I/O interfaces. All communications with the robot arm flow through the controller. Each joint is controlled with a dedicated microprocessor that communicates with the backplane computer for position inputs every 28 milliseconds. A servo drive system, positional feedback

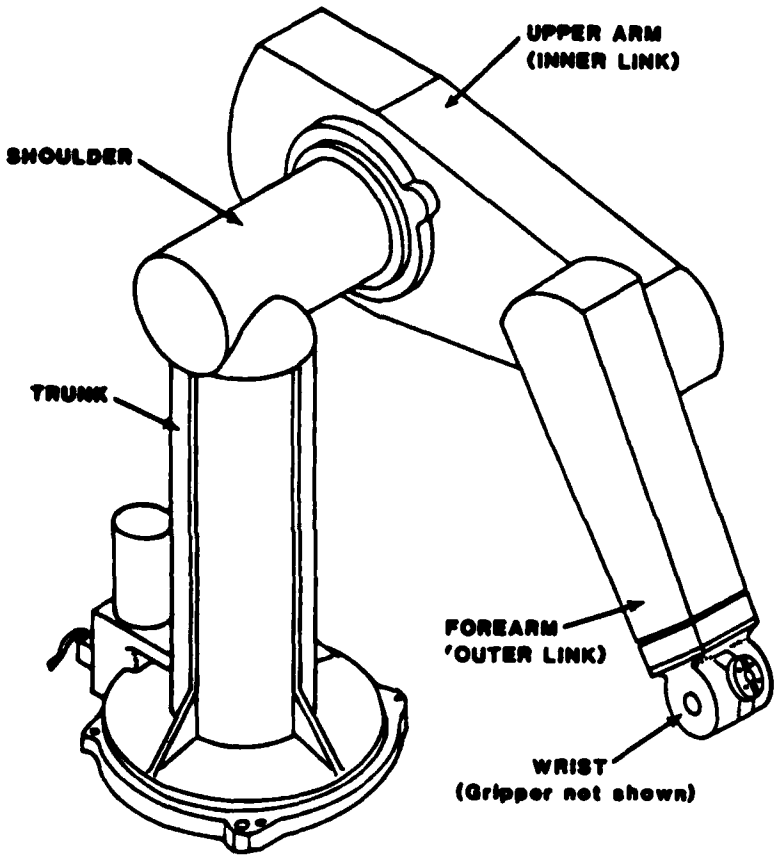

Figure 4. Robot Arm Link Identification [Ref. 3]

circuit and the microprocessor form the closed loop control system for each joint. The PUMA 560 robot system is delivered with a higher level language for programming [Ref.2].

The teach pendent and the terminal provide the primary input and output interface. They allow the operator to program the arm to perform various tasks. The program containing the task instructions is stored in non-volital memory in the controller memory. Additional storage and backup is provided on a magnetic floppy disk. An seperate I/O module allows synchronization of the arm with other equipment.

D. LIMITATIONS

The PUMA 560 industrial robot arm is 20 times the mass of its payload. This mass is necessary to provide structural stiffness and joint rigidity. For this ratio of payload to arm mass, rigid body assumptions in the equations of motion are valid. When the payload is increades, flexibility effects can lead to static position error. An increase in speed and acceleration will produce oscillations and tool overshoot. This tool overshoot often causes damage to the work-piece, tool and the robot wrist. As the payload and speed is increased, inertia effects will become more dominant and the resulting motion will be effected by the joint flexibilities. A primary objective of high performance robot development is to understand these flexibility effects and to integrate them into the equations of motion.

II. ERROR INDUCING FACTORS

Robot arms have traditionally been employed in pick and place operations where repeatability and resolution have been the prime concern. The teach and play-back programming method requires that the robot and plant equipment be set up prior to the programming. With the advent of higher level programming languages such as VAL II and the simulated teach capability of the CAD (Computer Aided Design) work stations, the advantages of off-line programming are recognized.

Link parameter errors, backlash, gear eccentricity and compliance of link joints all contribute to absolute positioning inaccuracies in robot arms. This error makes the off-line programming less precise than the teach and playback method. A study of the effects of each of these parameters on positioning accuracy is provided by Ahamad [Ref.1], and compensation techniques based on PID control are proposed.

Link parameter errors can contribute a significant error and their evaluation can be found in the literature. The effects of gear eccentricity are generally quite small [Ref.1:pg. 310] and their effect will be studied in future dynamic experiments.

Gear-lash effects are mainly observed because the joint sensors are located on the drive motor rather than the joint. When the direction of torque at a joint is changed we expect to

see a jump in the position -vs- load graph representing the effects of gear-lash.

Most industrial robots have flexible joints due to the torsional stiffness of the gear boxes and the drive shafts. Since the joint angle is measured at the drive motor the effect of this flexibility is a difference between the actual and desired joint angle when the arm is loaded. An estimate of this compliance will lead to compensation to correct the steady state positioning error. The torsional stiffness can also be factored into the equations of motion [Ref.4] and the resulting "small motion effects" that cause overshoot will be compensated in the dynamic control scheme. This accounting of the flexibility effects will allow the present robot arm to be safely run at enhanced performance levels.

III. FLEXIBILITY MEASUREMENTS

A. STATIC MEASUREMENTS

To determine the behavior of each joint to a torque load they will be isolated and tested individually. The drive motors for joints one, two and three contain motor brakes which lock the motors and thus the motor end of the drive trains. The wrist joint drive motors do not contain motor brakes and the individual drive trains are secured at the motor end of each drive shaft coupling using machined quills that extend through inspection holes to each coupling.

The joints will be subjected to a torque load that is approximately 150 to 200 % of the normal maximum torque load. The nominal load is modeled as a 2.5 Kg disk 10.2 cm in diameter mounted on the joint six flange. The specifications call for a maximum of 1.0 g dynamic acceleration at the load. It is a simple matter to convert this to a 49 Newton load at the flange (2 × g × 2.5 Kg) which represents the worse case of gravity acting in the same direction as the dynamic acceleration.

B. JOINT ONE RESULTS

Joint one (Figure 5) is driven by a DC servo-motor through two sets of spur gears, idler shafts and pinions which drive the bull gear. The two idler shafts have different torsional rigidities.

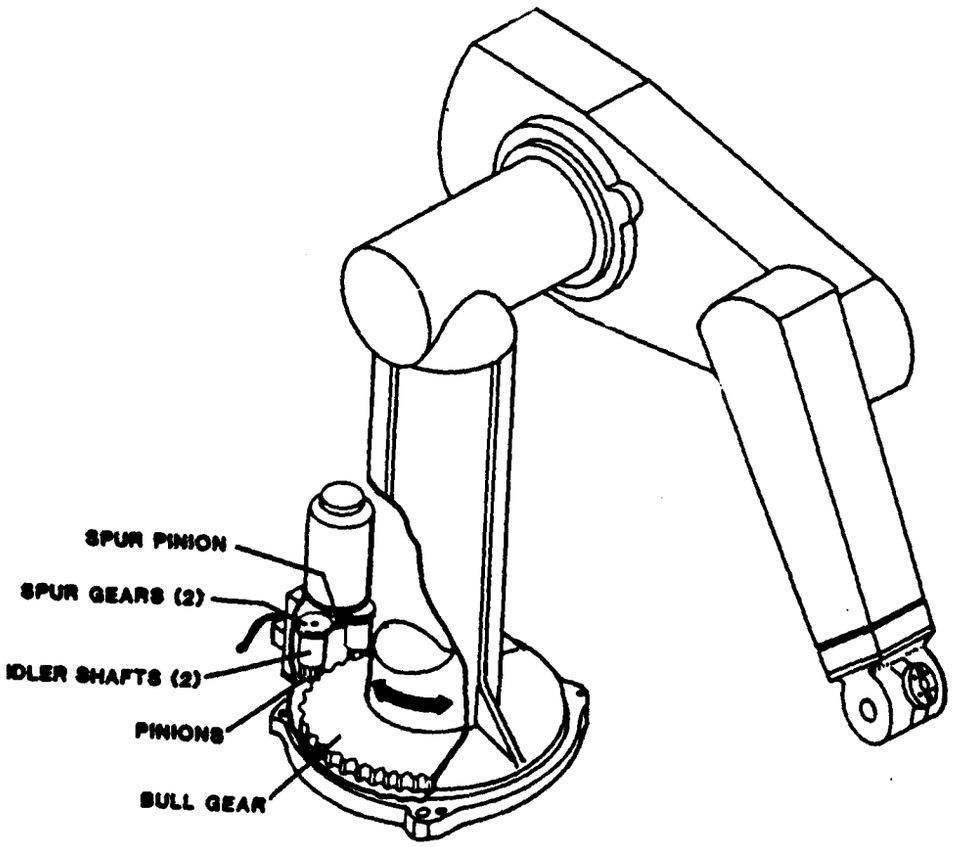

Figure 5. Joint One Gear Train [Ref. 3]

The shaft that has high torsional rigidity prevents appreciable twisting and provides good structural stiffness for the joint torque transmission. The other shaft has a lower torsional rigidity designed for a predetermined amount of windup to preload the entire gear train eliminating backlash. In Figure 5 we see that the bull gear rotates the arm via a large cylindrical column which rotates relative to the base Assembly.

To measure joint flexibility (Figures 6 and 7), a test was carried out on joint one by loading in the counterclockwise (CCW) sense (as seen from the top down) and then incrementally reducing the CCW load and increasing the load in the clockwise (CW) direction. When the CW loading was complete, the process was reversed for a total of six loading cycles. The data is summarized in (Table 1).

The (Table 1) data plotted in Figure 8 shows a break at 33.9 N-M in the CW direction with a nominal magnitude of .0024 radians (0.14 deg.). This break is the gear lash produced when the torsional preload was overcome. The data clearly shows a hysteresis loop which is the effect of the dissipative effects of friction in the drive line.

Concentrating on the data below 33.9 N-M in the CW direction as graphed in Figure 9, the remaining data points are essentially linear. The slope of the line generated by the linear interpolation scheme represents a joint flexibility of 1.47×10^{-5} Rad/N-M. This equates to a joint spring constant of 68,000 N-M/Rad.

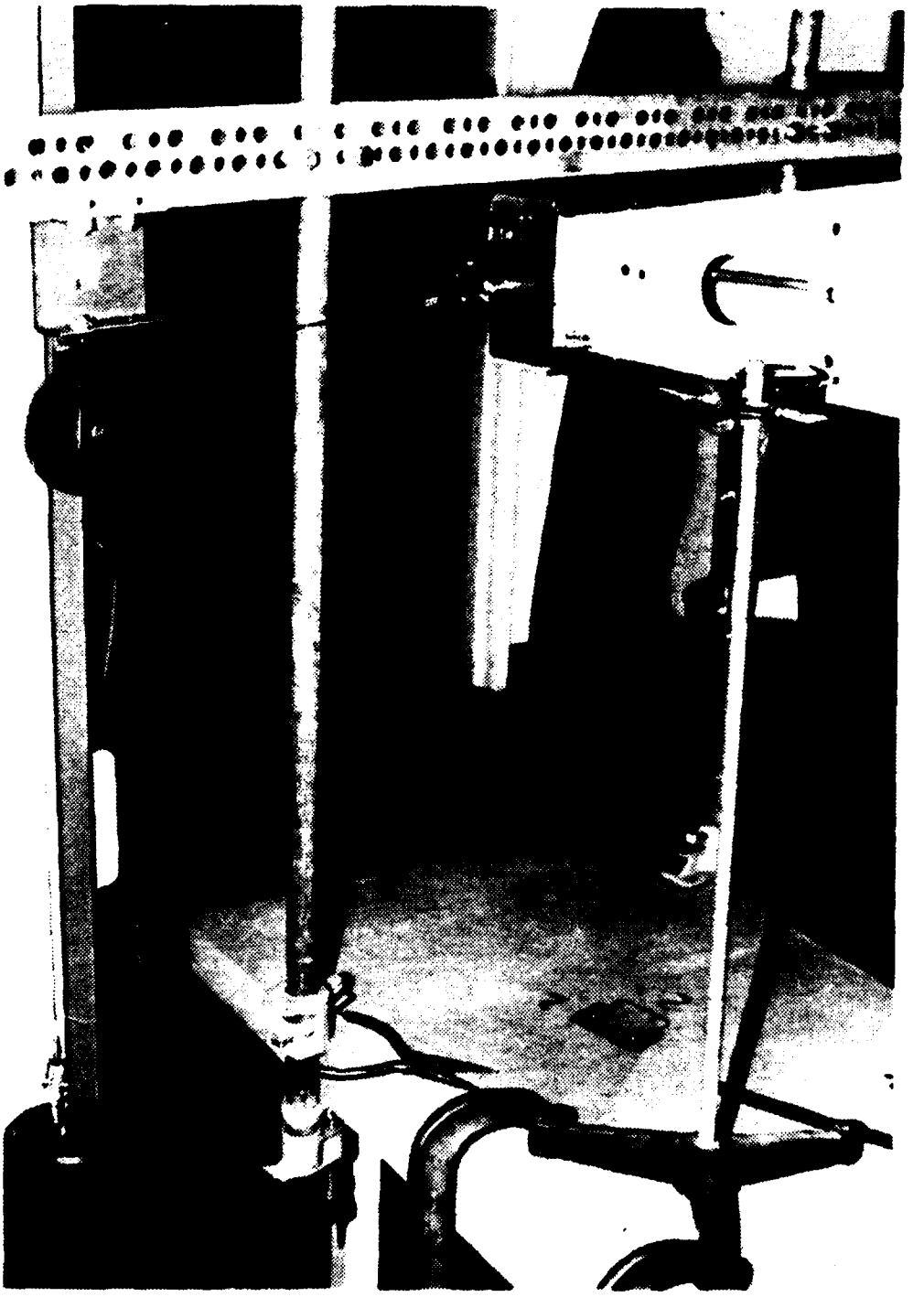

Figure 6. Joint One Experiment (CCW)

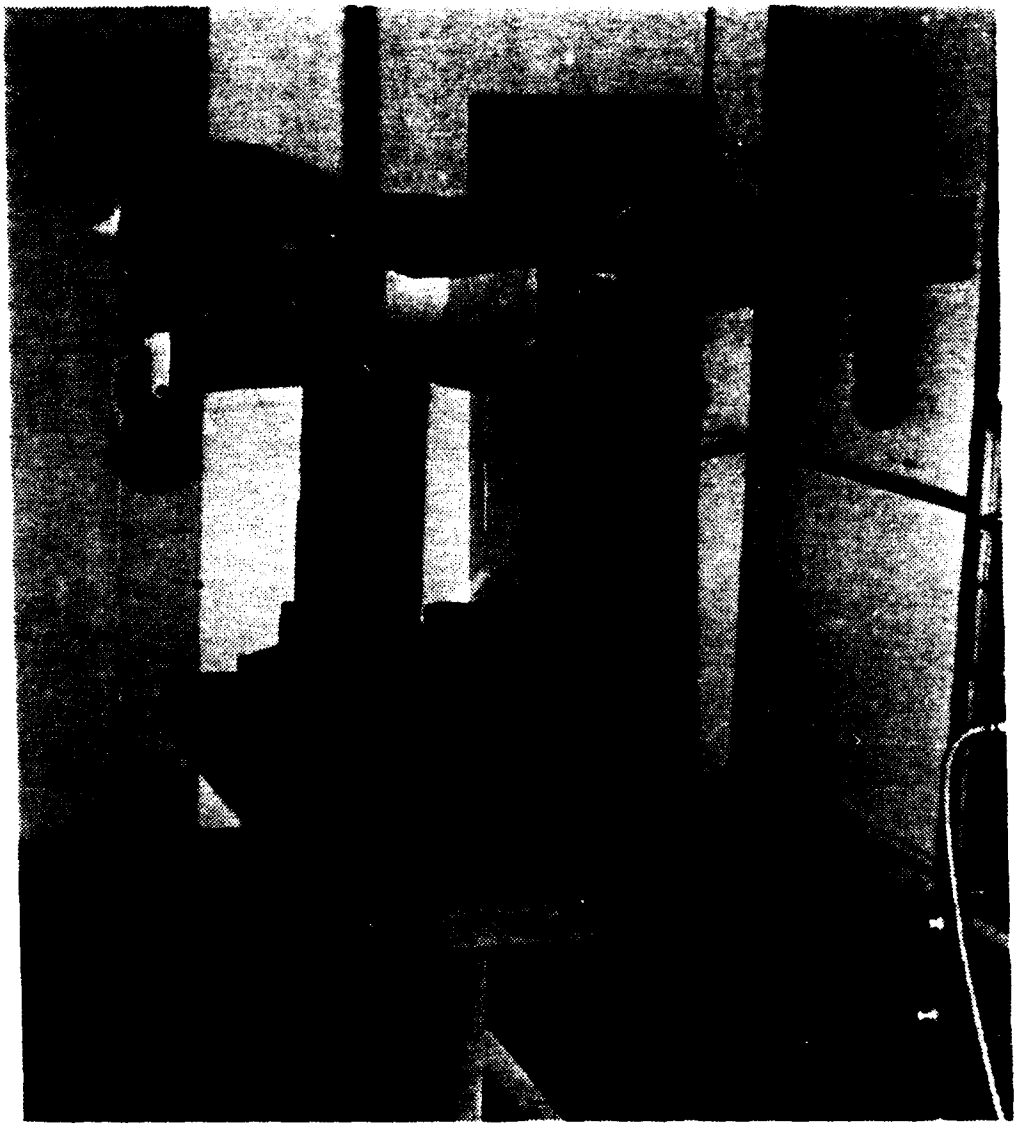

Figure 7. Joint One Experiment (CW)

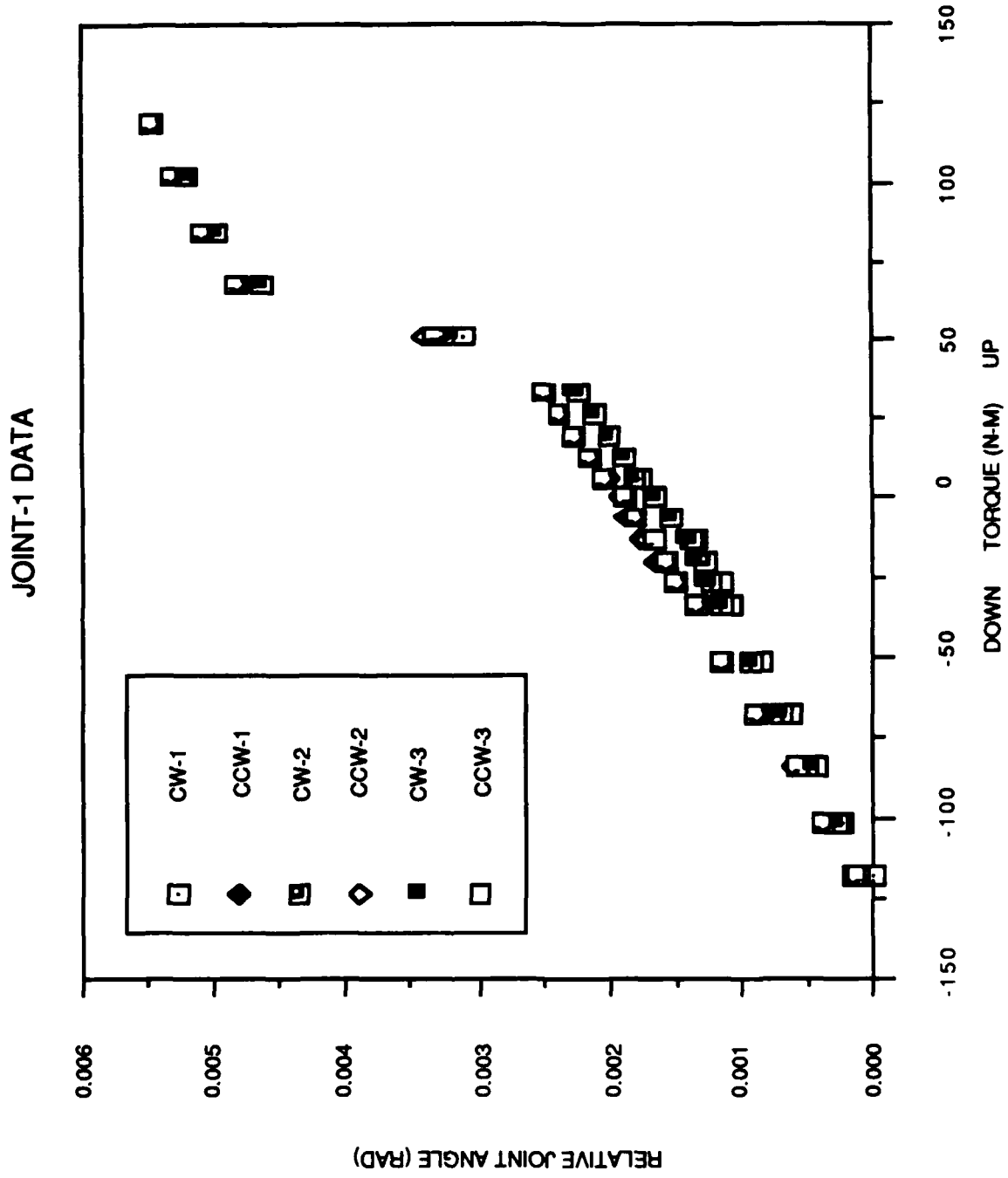

Figure 8. Joint One Data

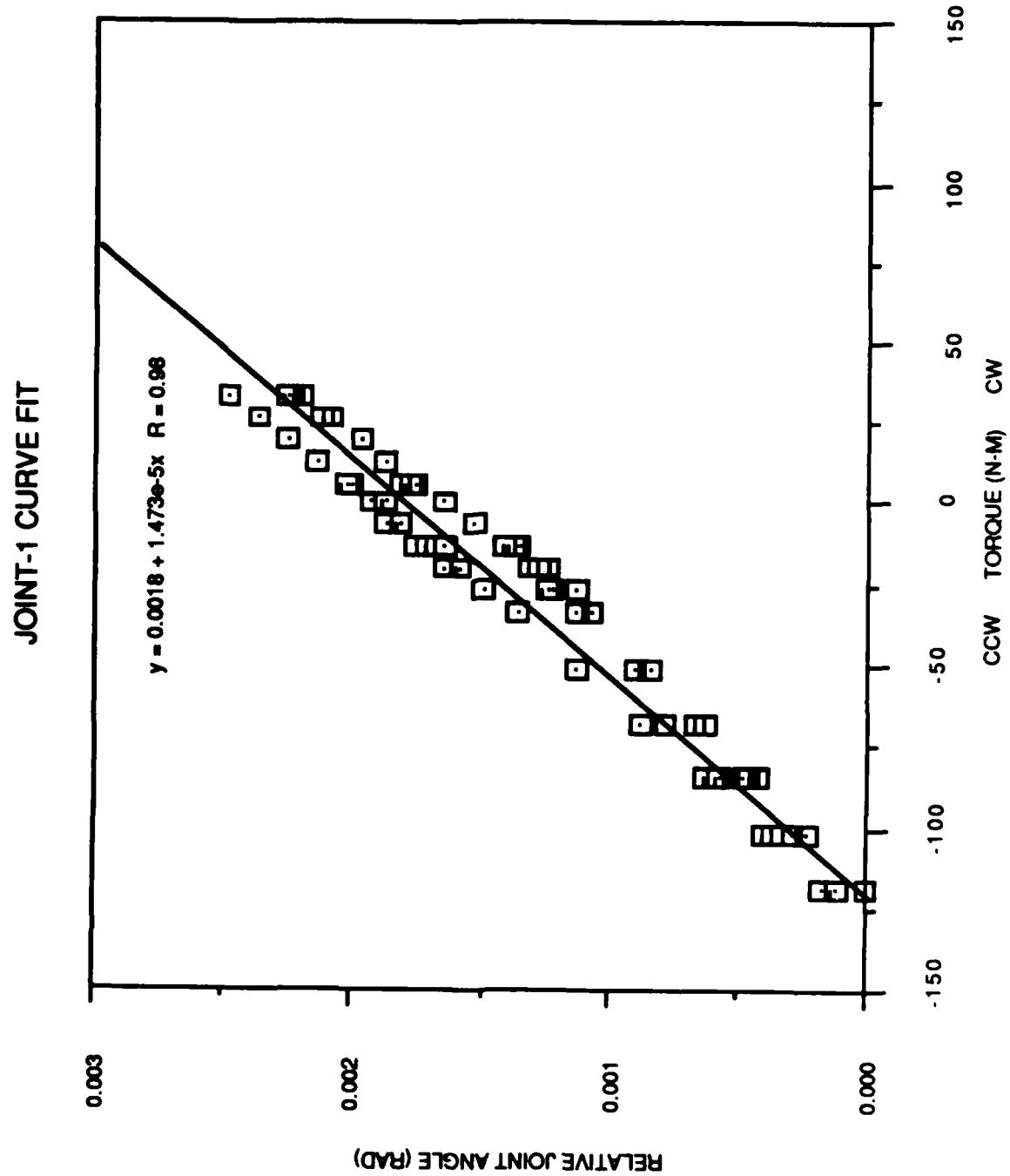

Figure 9. Joint One Curve Fit

The value of 33.9 N-M represents 150 % of the maximum torque at rated load and speed. The existence of the break in the CW sense at 33.9 N-M could pose problems in path deviations when the arm is operated in a region of increased performance. There are perhaps two solutions to this problem. The first would be to increase the preload which would result in increased gear wear and increased friction loads, both of which must be avoided in a production machine. The second solution is to control the rate of acceleration to stay within the linear range.

C. JOINT TWO RESULTS

Joint two (Figure 10), uses a bevel gear set to drive a spur pinion around a shoulder fixed bull gear. Gear lash compensation is accomplished by providing a gear-interface adjustment at each gear pair. The adjustment provides sufficient latitude to zero out gear-lash over the working life of the drive train.

To measure the flexibility at joint two (Figure 11), a fixture was manufactured which allowed the joint to be loaded down directly with weights and to be loaded up through a set of two pulleys. An angle piece along the centerline of the link at the outer end allowed the deflection to be read with a dial indicator. The joint was loaded initially in the downward direction. The weight was incrementally reduced to zero and then increased in the up direction until the joint was fully loaded. The load sequence was reversed for the second cycle and a total of six cycles were performed. The data is summarized in (Table 2).

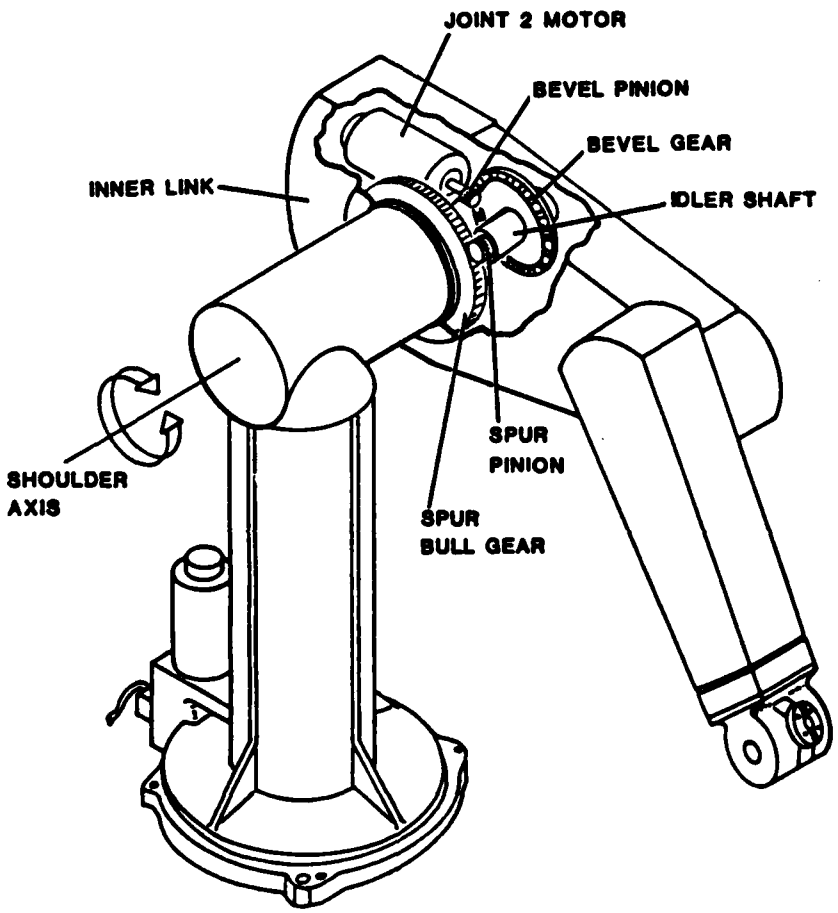

Figure 10. Joint Two Gear Train [Ref. 3]

Figure 11. Joint Two Experiment

The (Table 2) data plotted in Figure 12, behaves in a linear fashion with evidence of slight hysteresis. The hysteresis is caused by dissipation of energy due to friction effects in the drive train. The joint two curve fit (Figure 13) gives us a joint flexibility of 1.503×10^{-5} RADS/N-M or a joint spring constant of 66,500 N-M/RAD.

There is no evidence of the effects of gear lash in the data. It is also notable that the range of the test torque is ± 70 N-M while the full load torque on joint two during normal operation is 45 N-M (2.5 Kg × 2g × .92m). Thus the joint behaves in a linear fashion up to 155% of system load.

D. JOINT THREE RESULTS

The joint three drive train (Figure 14) has a gear train similar to joint two with the exception that the motor is linked to the gear train via a drive shaft and helical spring couplings. Gear lash compensation is similar to that provided in joint two.

To test joint three, the inner link (Figure 15) is bolted to the frame using a steel column. This ensures that the deflection read at the dial indicator is a result of joint three deflection and not that of joint two and three. A collar was fabricated and bolted to the outer link providing attachment for the weights and a centerline reference for measurement. The link is first loaded in the down direction the the load is cycled in the same manner as in the joint two experiment. The maximum torque load at joint three in normal operation is 22.6 N-M (2.5Kg × 2g × .46m). The

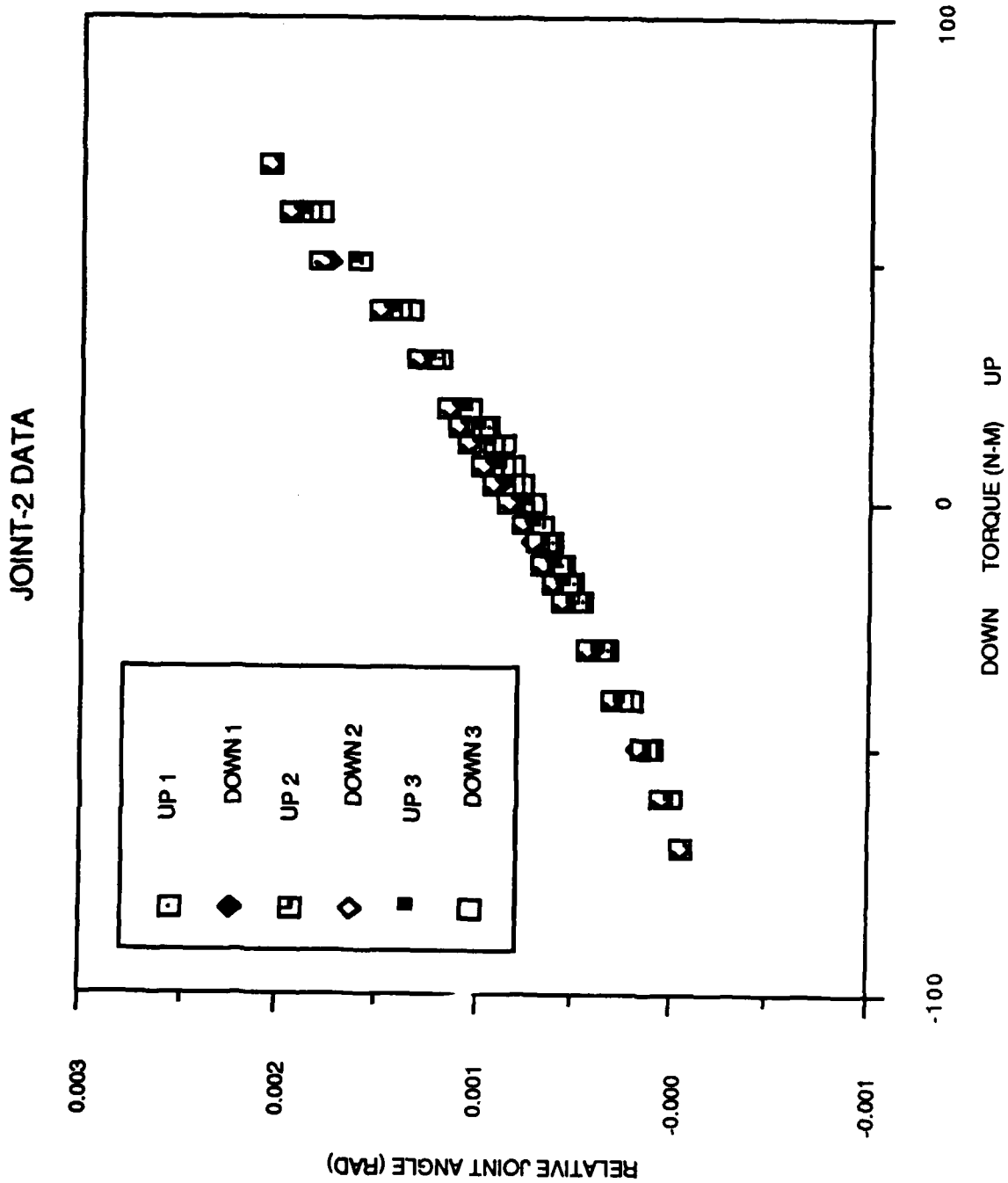

Figure 12. Joint Two Data

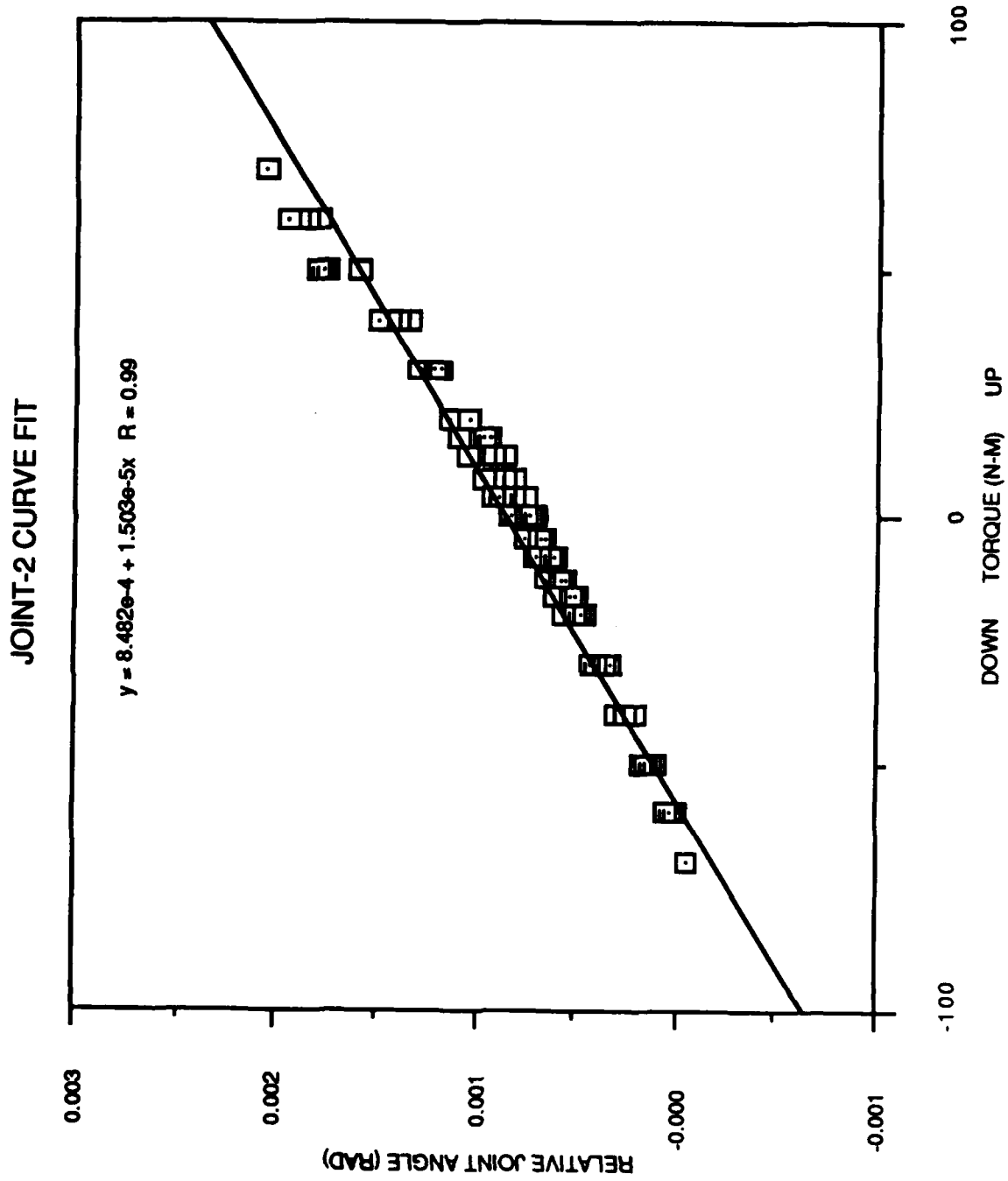

Figure 13. Joint Two Curve Fit

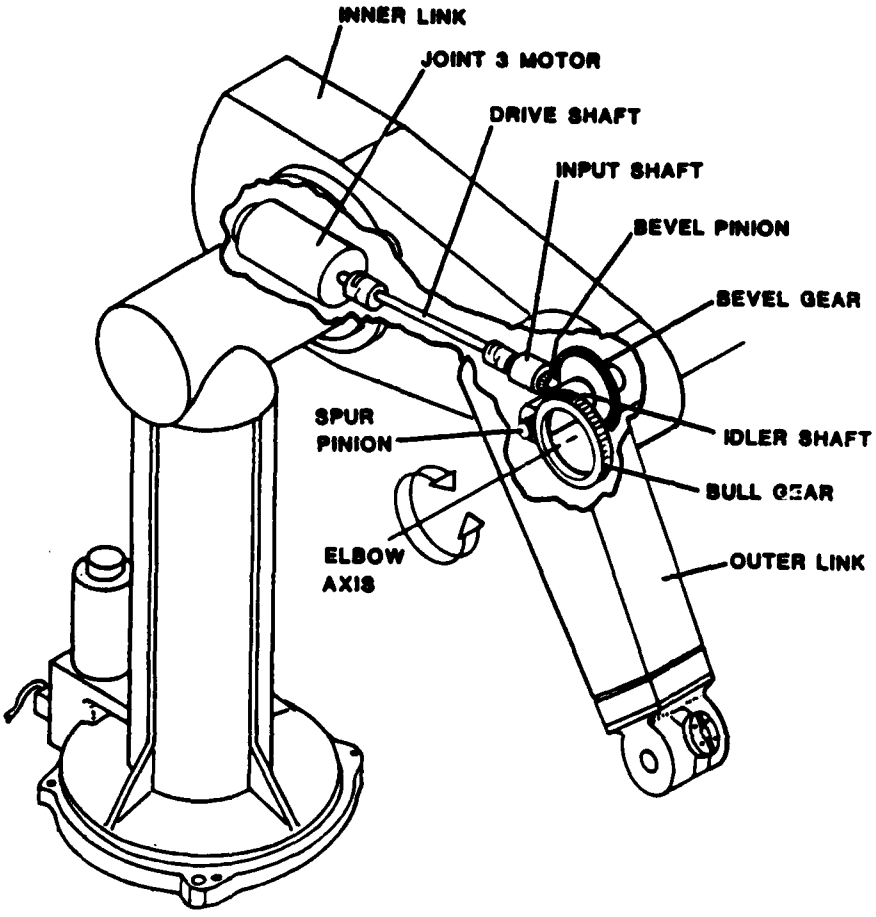

Figure 14. Joint Three Gear Train [Ref.3]

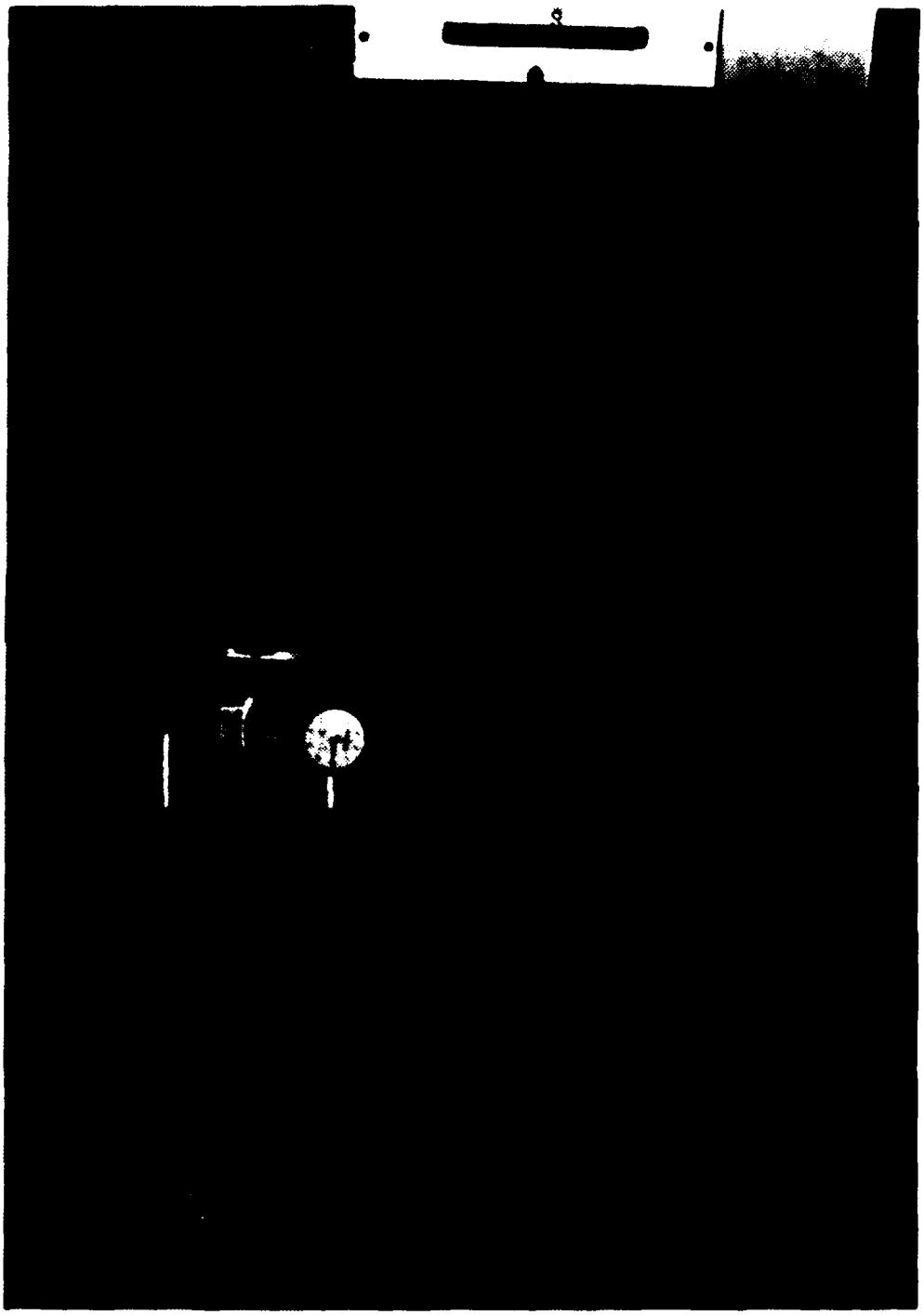

Figure 15. Joint Three Experiment

experimental applied torque of 40.6 N-M represents a load at 185 % of the maximum.

The data obtained from joint three (Table 3), plotted in Figure 16, clearly shows a linear relationship and exhibits a hysteresis loop. There are no steps in the data to suggest gear lash effects. With reference to Figure 17, the joint flexibility is 8.585×10^{-5} RAD/N-M and the joint torsional spring constant is 11,650 N-M/RAD. This represents a six-fold decrease from the spring constants of joints one and two. There are two primary reasons for this, the first is the reduction in physical size for the gear trains and their supporting structures and the second is the effect of the spring coupling flexibilities.

E. JOINTS FOUR, FIVE AND SIX

The articulation of the wrist is accomplished by joints four, five and six (Figure 18). Their respective drive motors are located at the opposite end of the outer link and the torque is transmitted from the motors to the gear trains through drive shafts with helical spring couplings at each end. Joint four, wrist rotation, is driven through two sets of spur gears. Joint five, wrist bend, is driven through first a spur gear pair and then a bevel gear pair. Joint six, flange rotation, is driven through two sets of bevel gears. All of the gear trains have backlash compensation adjustments which change the shaft centerline distances as in joints two and three.

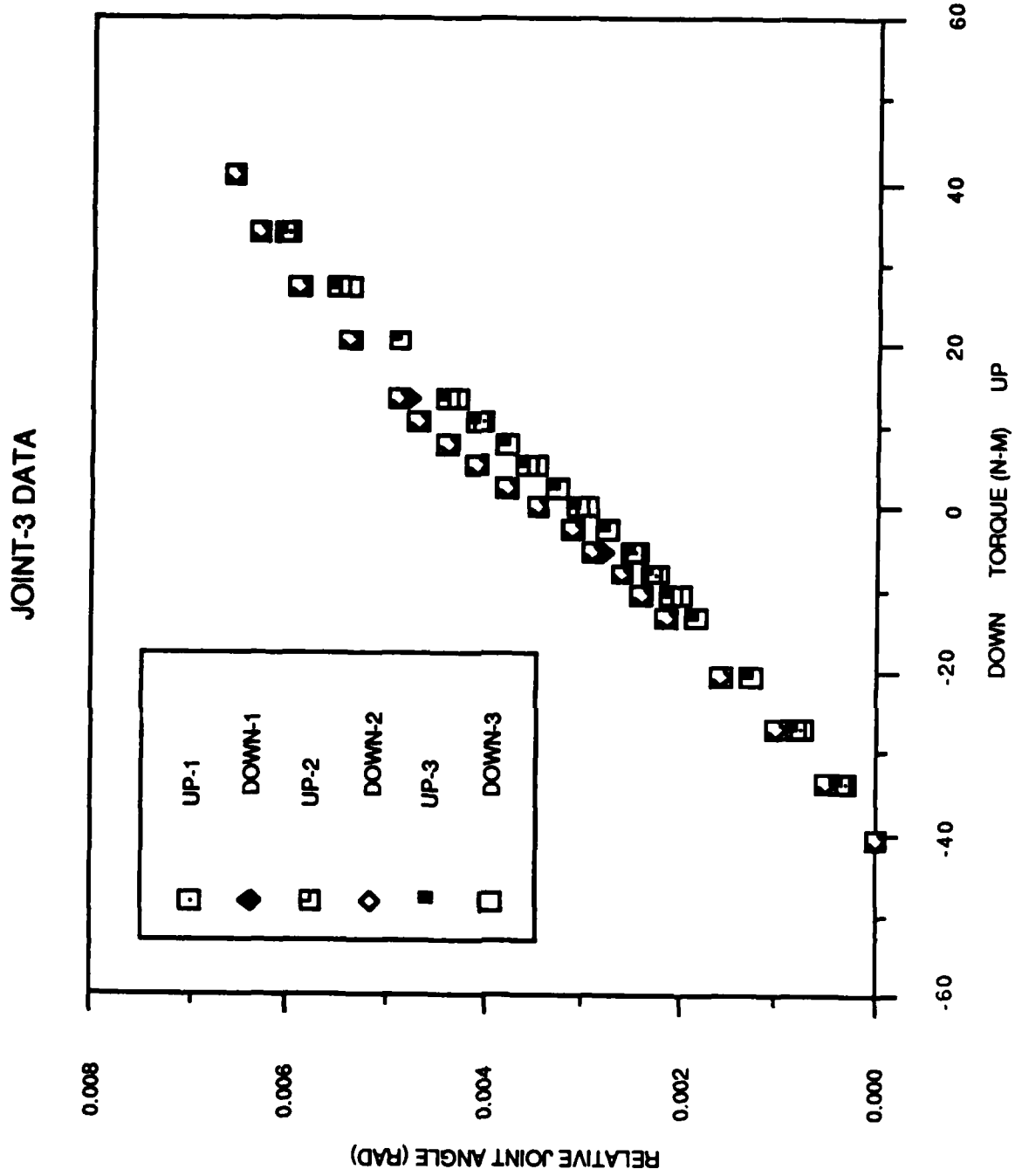

Figure 16. Joint Three Data

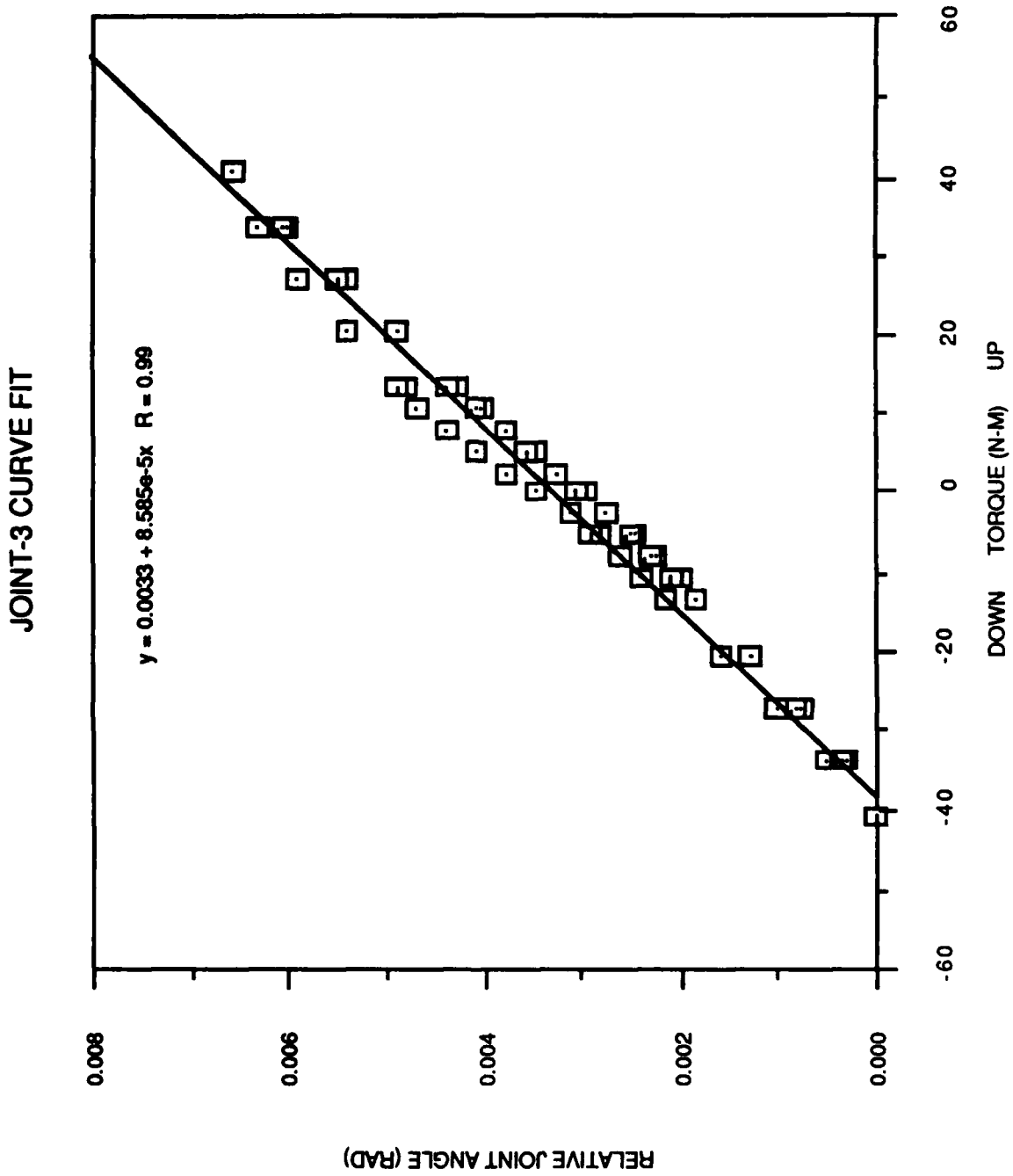

Figure 17. Joint Three Curve Fit

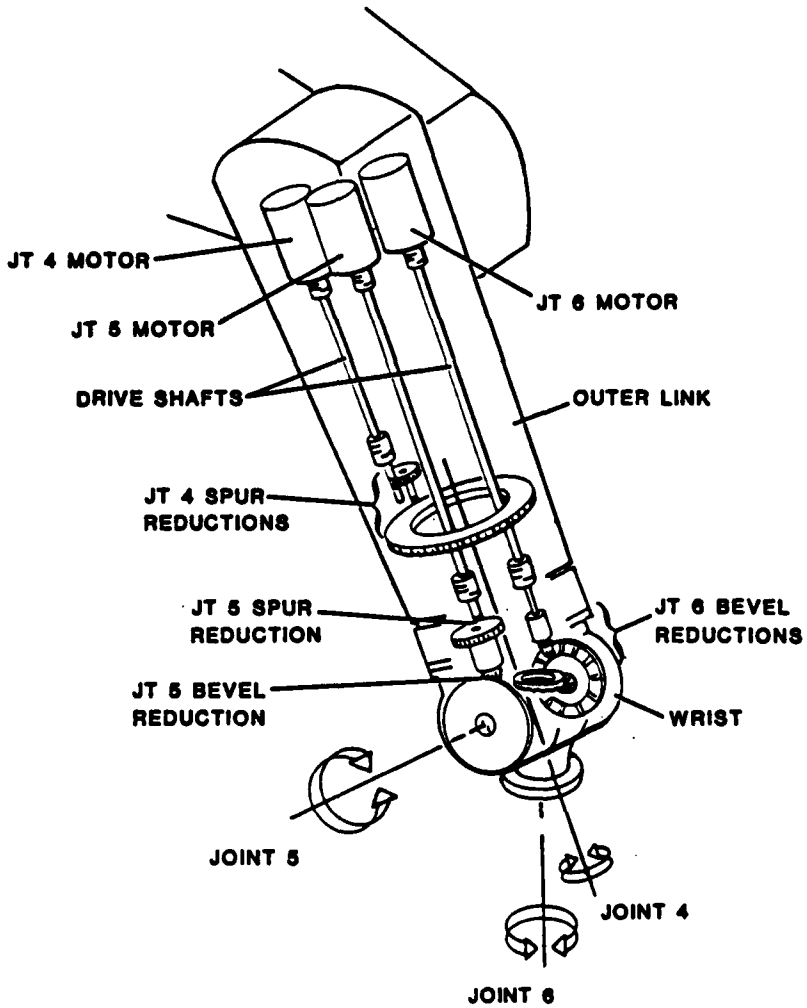

Figure 18. Wrist Articulations Joints Four, Five and Six [Ref. 3]

To test joint four (Figure 19), the inner and outer links are bolted to the frame. The flexible couplings are pinned to the link structure at the motor ends so that the flexibility measured is that of the entire drive train. This pinning is accomplished with long quills that screw into the coupling fastener hole and pass through the frame through the disassembely access holes. An Assembly that allows weights to be placed to develop a torque about the joint four axis has been fabricated and clamped in place. The test was preformed by loading the joint in the CCW direction and incrementally reducing the load and increasing it in the CW direction. This procedure was performed for a total of six cycles.

The data in (Table 4), plotted in Figure 20 is again essentially linear but exhibits a greater variation in the slope of the data than previous joints. Since the flexibility is composed of the sum of all the flexibilities in the system this behavior can be attributed in part to the relative smaller size of the joint four drive train. The frictional effects are again present as evidenced by the hysteresis present in the data. The flexibility (Figure 21) is 4.652×10^{-4} RAD/N-M and the torsional spring constant is 2150 N-M/RAD. This is again a significant drop form the value of 11,900 N-M/RAD found in joint three.

The test for joint five is similar to the test for joint four The drive train is pinned to the frame at the motor end of the helical spring coupling. Figure 22 shows the apparatus which consists of a pipe that extends out from the manipulator mounting flange providing a lever arm and a radius to measure deflection.

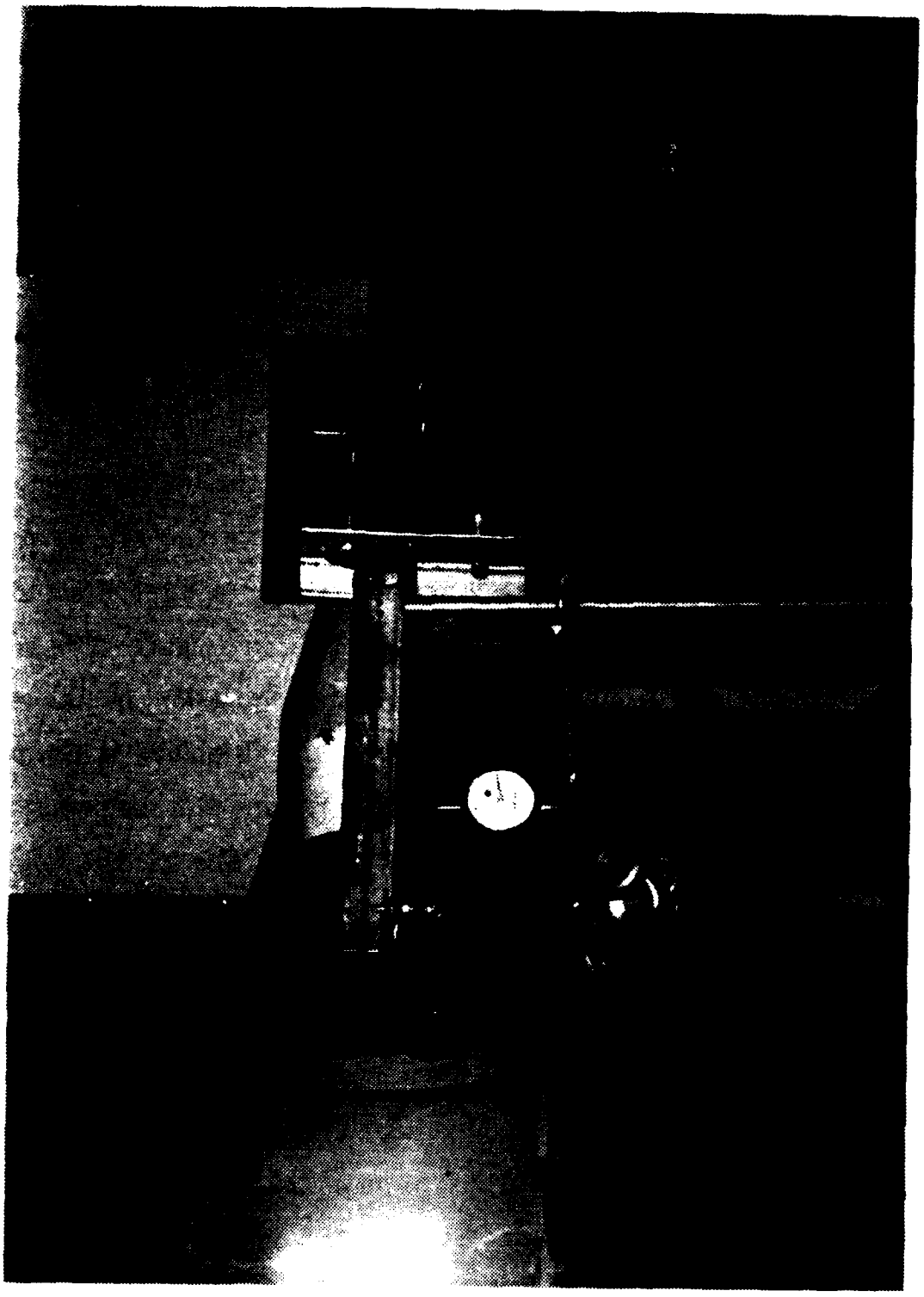

Figure 19. Joint Four Experiment

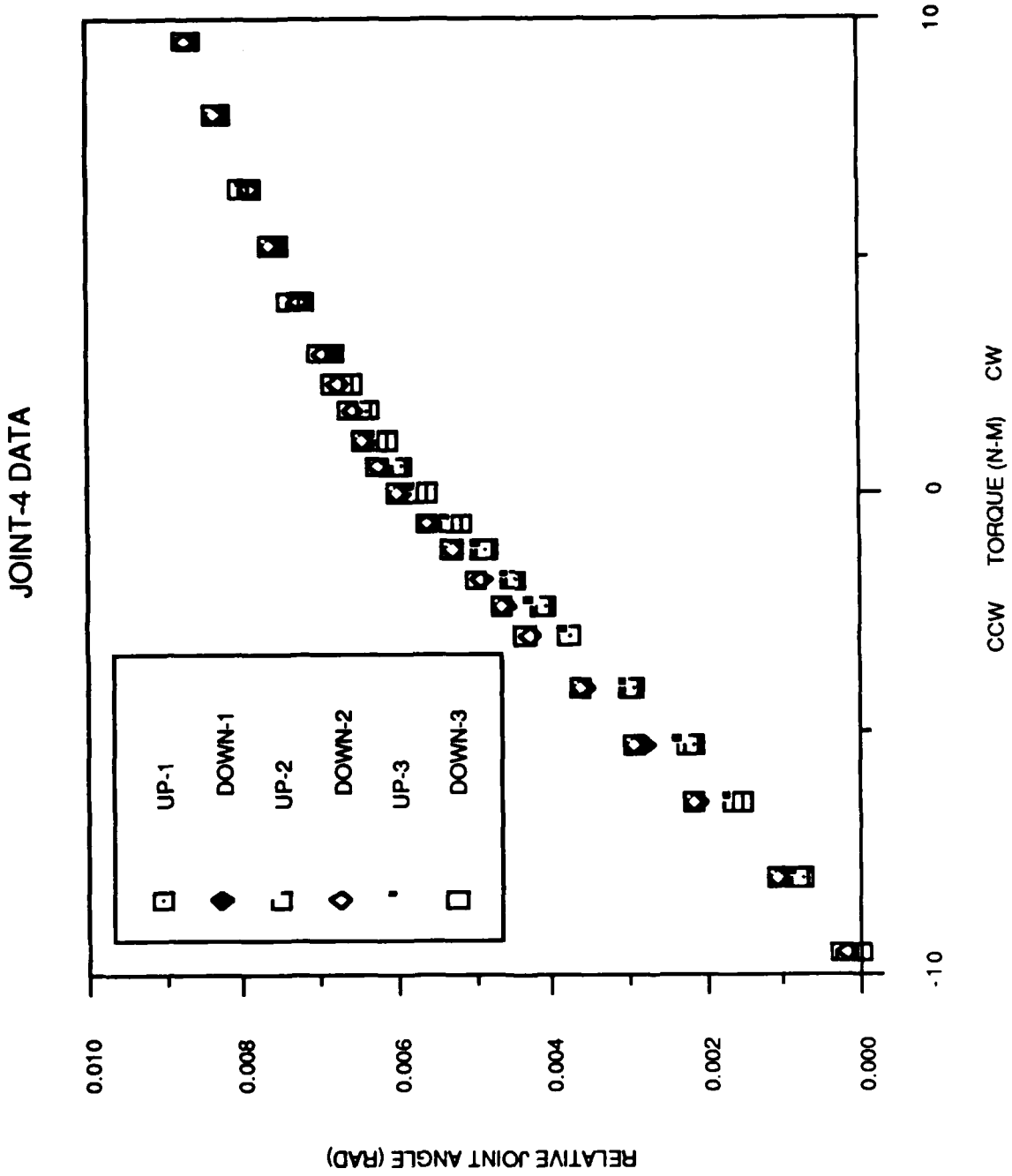

Figure 20. Joint Four Data

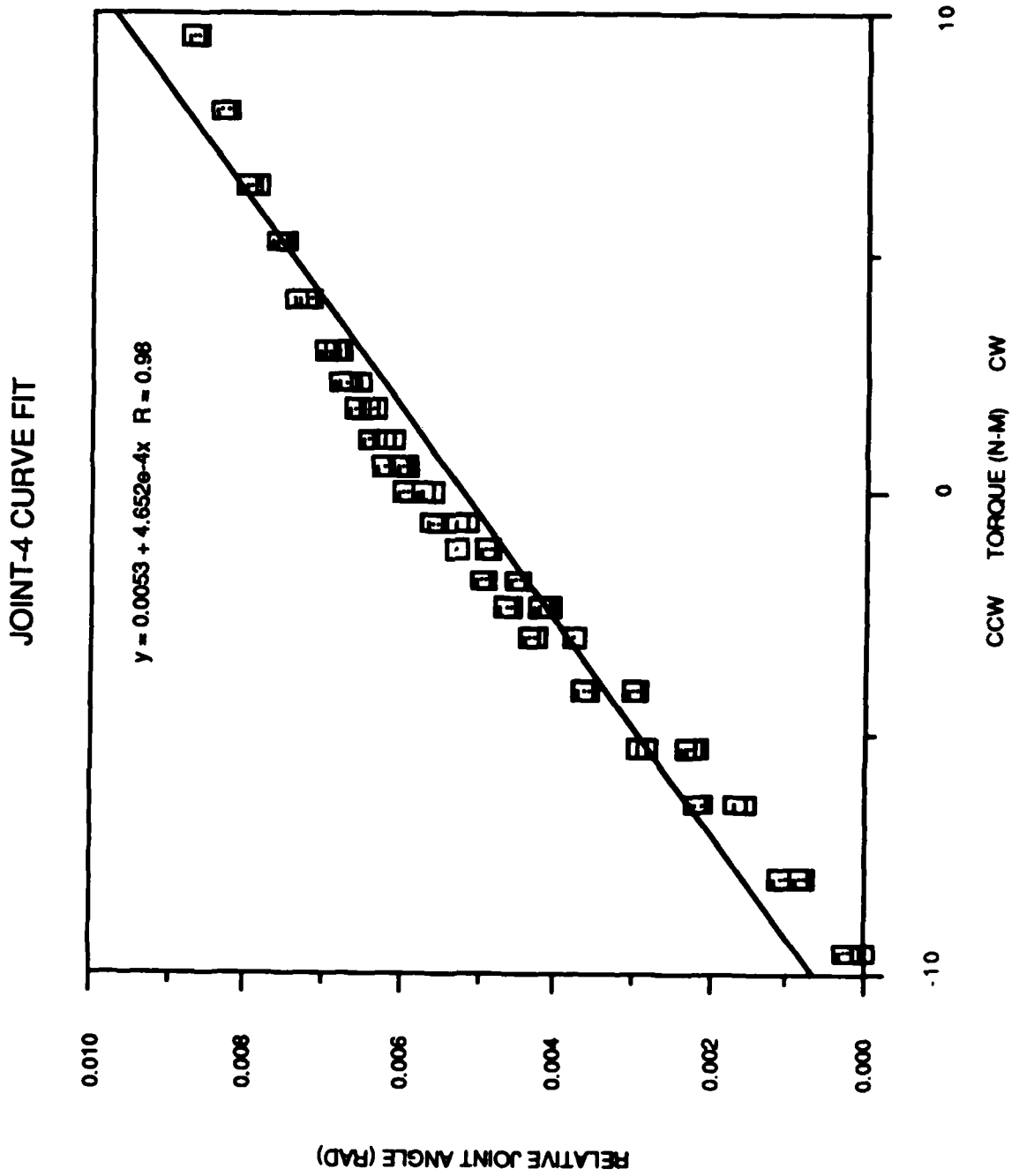

Figure 21. Joint Four Curve Fit

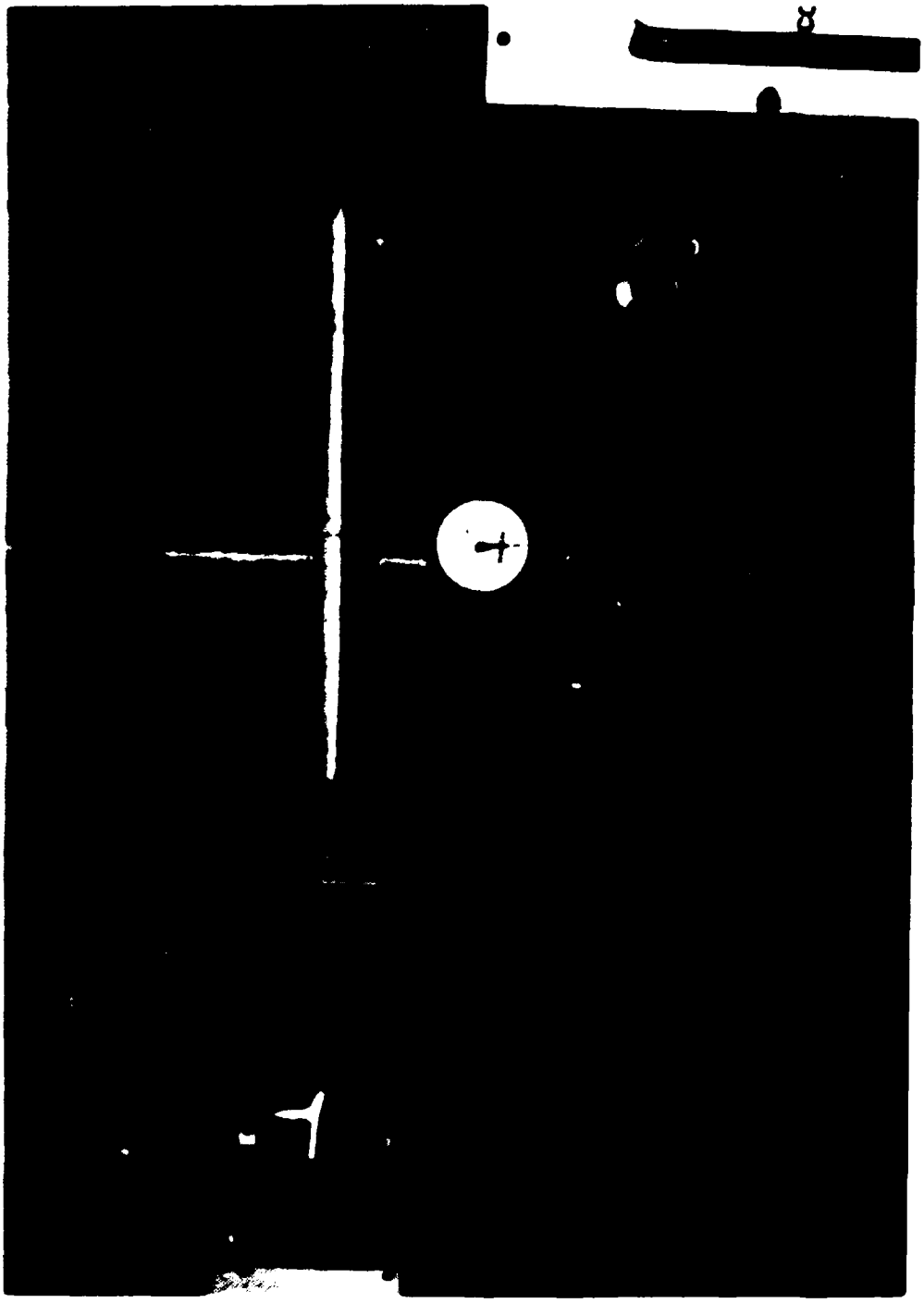

Figure 22. Joint Five Experiment

The wrist has been rotated about joint four so that the rotation about joint five is in the plane of Figure 22. The collar bolted to the base of the wrist has two set screws on each side to restrain movement about the joint four axis.

The data in (Table 5), and plotted in Figure 23 was taken by first loading the joint in the down direction, incrementally reducing the load to zero and loading in the up direction with the pulley arrangement. The loading was then reversed and the joint returned to the original loading. This cycle was repeated three times for a total of six sets of data points. The resulting data behaves in a relatively linear fashion and shows evidence of a slight hysteresis loop. Figure 24 shows that the curve fit for the data indicates a joint flexibility of 8.828×10^{-4} RAD/N-M and a joint spring constant of 1130 N-M/RAD. This value is very close to that of joint four which reflects the similarity of the two drive trains.

For the joint six test (Figure 25) the wrist is rotated 90 degrees about joint four so that the plane of rotation for joint five is horizontal. The flexible couplings for joints four, five and six are all pinned to the outer link frame at the motor ends. A square beam is attached to the manipulator mounting flange in the horizontal position so that weights can produce CW and CCW torque loads about joint six. The beam also provided a radius for the dial indicator to measure deflection.

The joint is preloaded in the CCW direction. The weights are then incrementally reduced and reapplied to produce a torque in

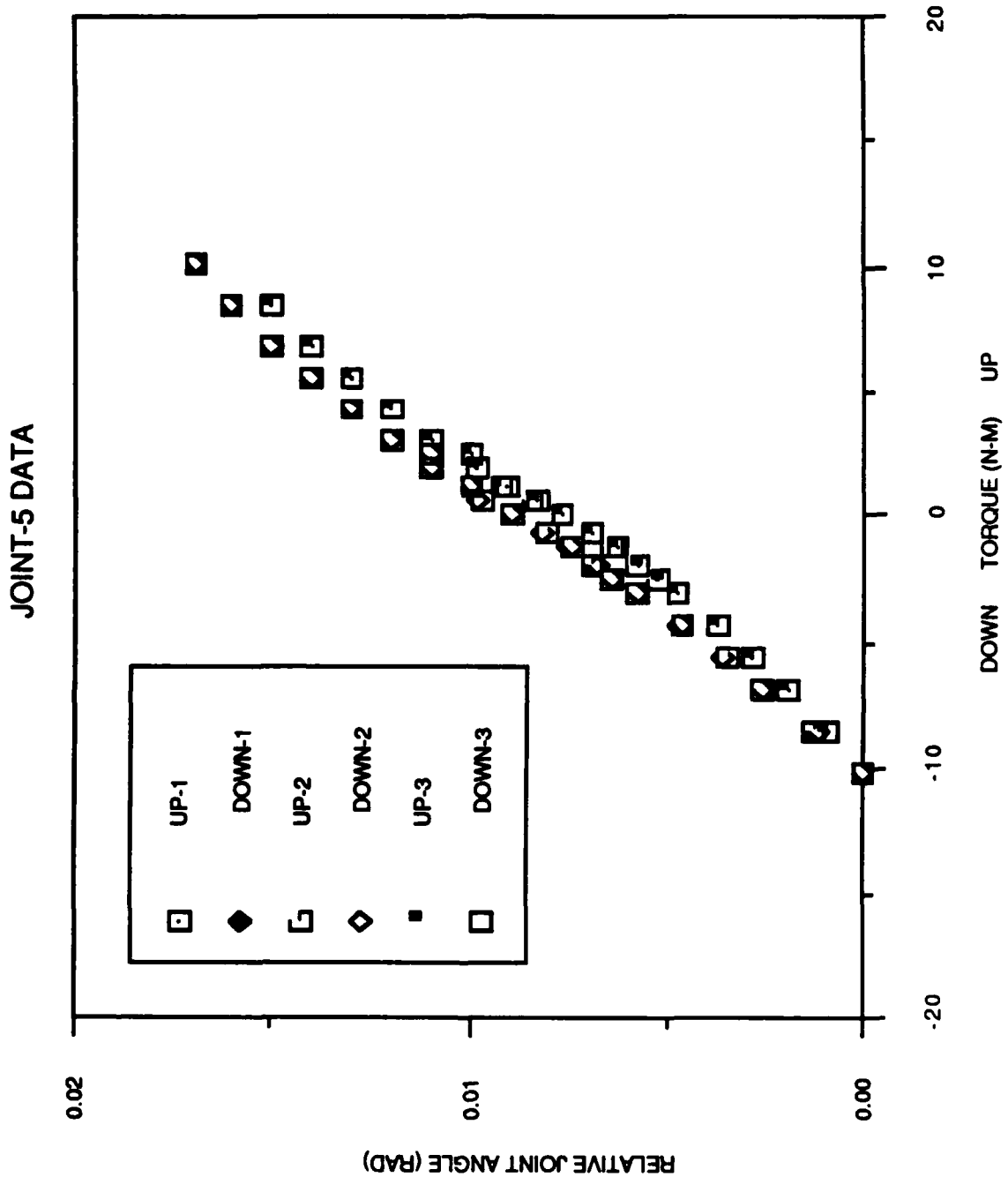

Figure 23. Joint Five Data

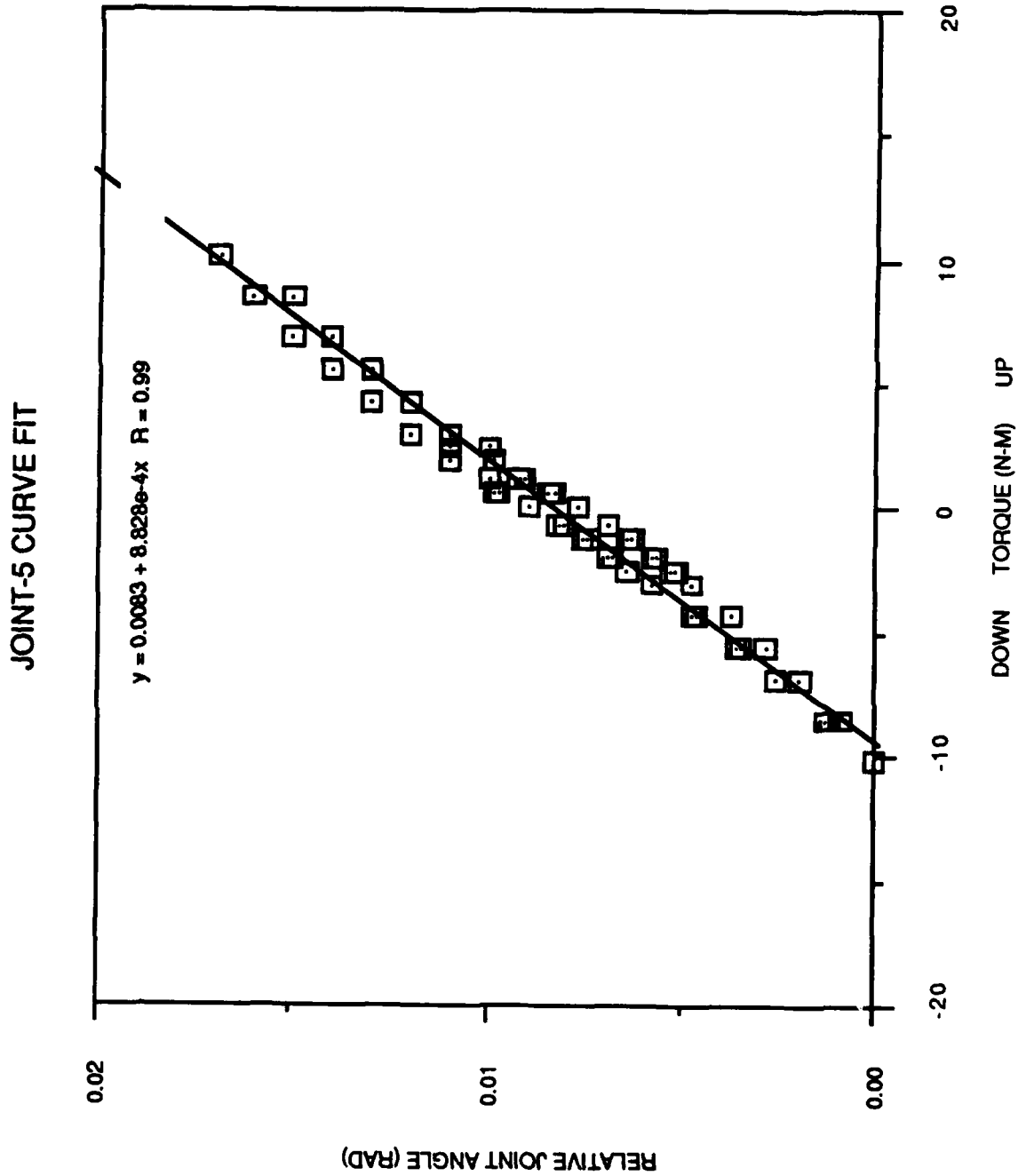

Figure 24. Joint Five Curve Fit

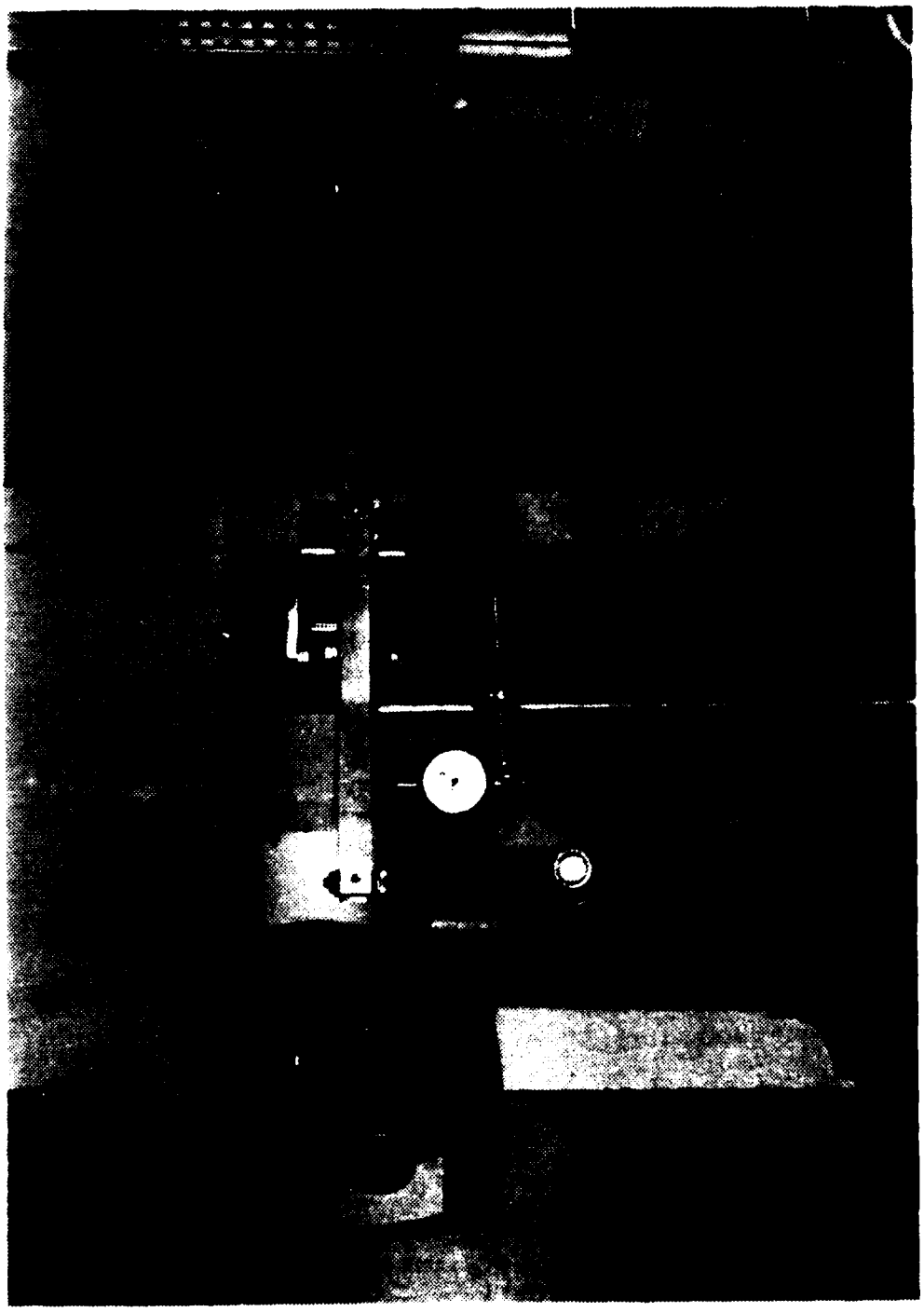

Figure 25. Joint Six Experiment

the CW direction. This procedure is repeated until the joint returns to its original CCW loading. The procedure is repeated three times producing six data sets.

The data in (Table 6) and plotted in Figure 26 again shows a linear behavior with dissipative friction effects producing a hysteresis loop. A look at the curve fit (Figure 27) shows a joint flexibility of 5.957×10^{-4} RAD/N-M and a joint torsional spring constant of 1680 N-M/RAD. This value is slightly stiffer that the two previous joints.

While the three joints in the wrist share similar drive trains differences in the actual gear trains and variations in the amount of force used in the gear lash compensation mechanisms can account for different spring constants. Overall, the torsional spring constants for the wrist joints are much smaller than those of the first three joints.

F. DYNAMIC MEASUREMENT

To measure the error between the indicated and actual joint angle the PUMA 560 joints must be instrumented. The problem of instrumentation has been investigated and the long lead time hardware is on hand to complete the job.

The measurement of the joint angle directly with an incremental shaft encoder is not feasible because encoders presently available do not have the resolution to the system resolution of .005 degree. A direct reading incremental shaft encoder would need 18,000 divisions per revolution read in quatrature to produce

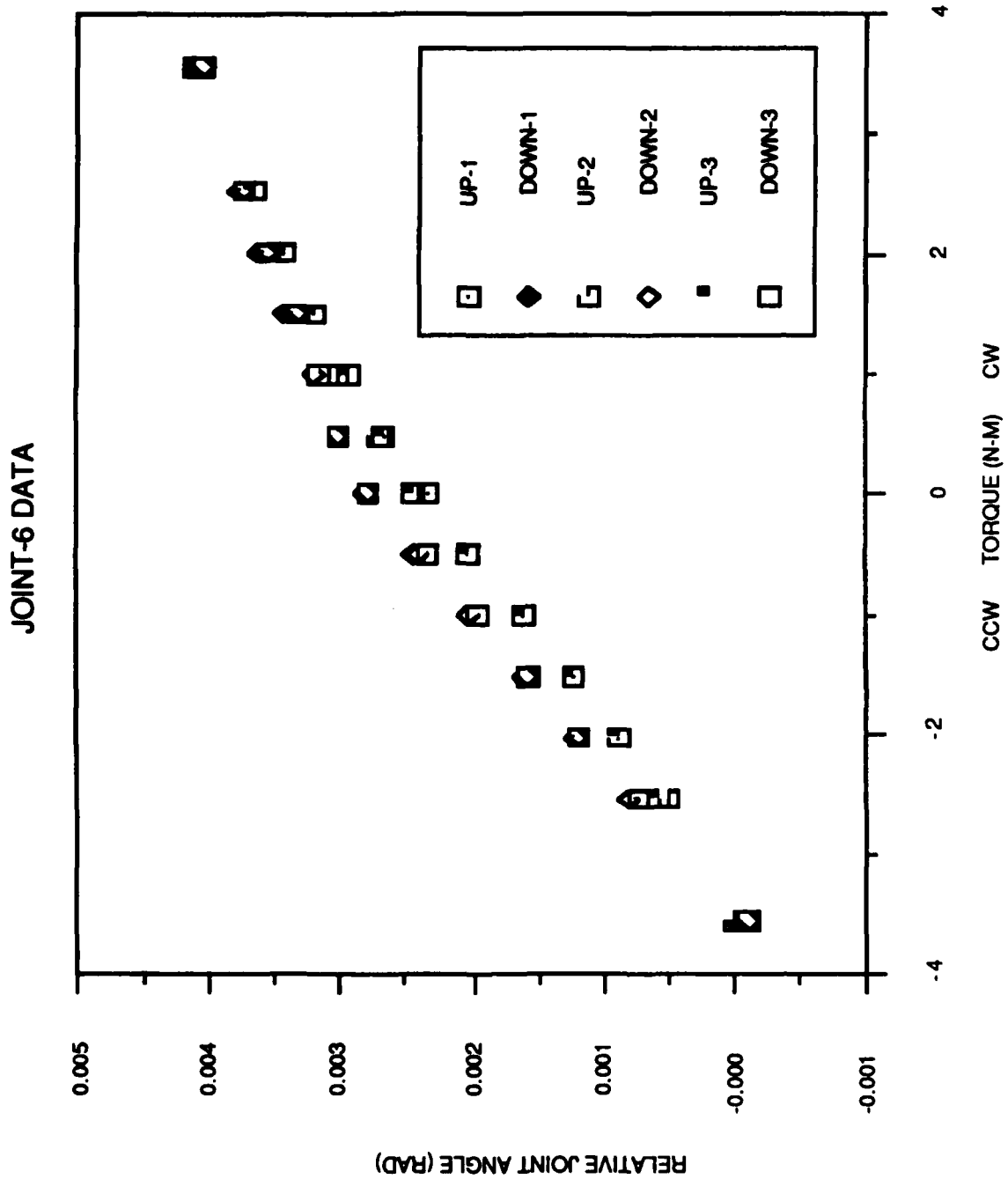

Figure 26. Joint Six Data

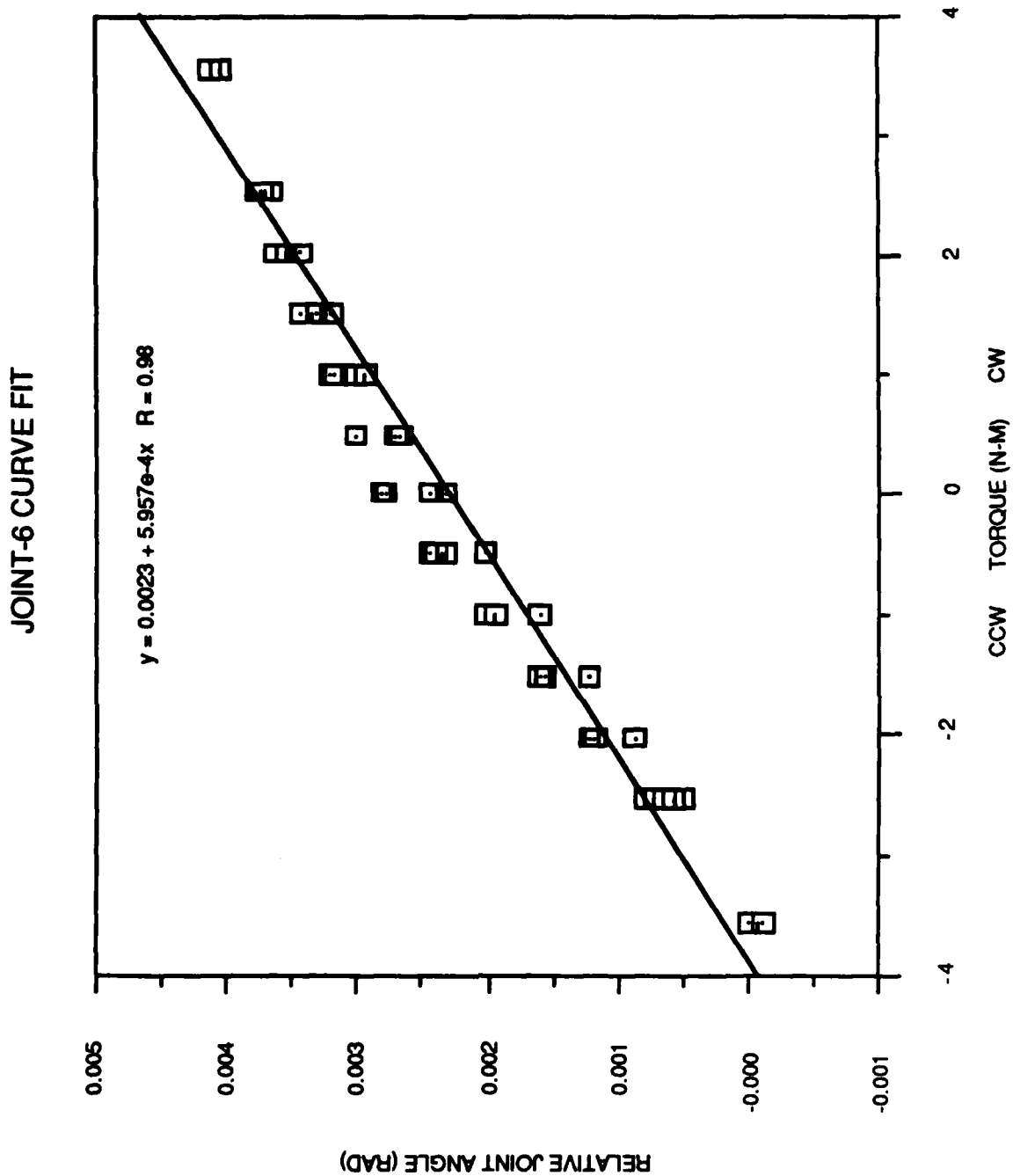

Figure 27. Joint Six Curve Fit

this resolution [Ref.5]. The results of the static testing has shown that for joints two through six, gear lash is not present. This leaves the option to insert the encoders in the existing gear train to take advantage of favorable gear step-up ratios.

Joint one (Figure 5) will be relatively difficult to instrument. The gear teeth on the base circle are not readily accessable [Ref.6] and a direct gear drive to an encoder may not be an acceptable solution. An encoder positioned at the base circle will not reflect flexibilities of the joint one torsional column. An alternative to a gear driven encoder at the base may be an encoder positioned near the top of the base pedestal driven by perhaps a friction drive. The problem of instrumentation of joint one will require careful consideration of both the arm construction and the precise transmission of motion to the encoder.

In joint two (Figure 10) and joint three (Figure 14), the outside face of the bevel gears is accessable through the inner link cover (Figure 28). The two dark circular covers are press fit rubber covers that protect the bevel gear from foreign matter. With the covers removed, the back of the bevel gears are exposed and provide access to mount an encoder to turn at the same rate as the bevel gear.

Instrumenting the wrist will involve accessing the various gear trains. The precise location of these access will have to be determined with further investigation and wrist disassembly.

The incremental encoders will be interperated by an IBM PC-AT using interface boards. The boards (four of them) fit in the

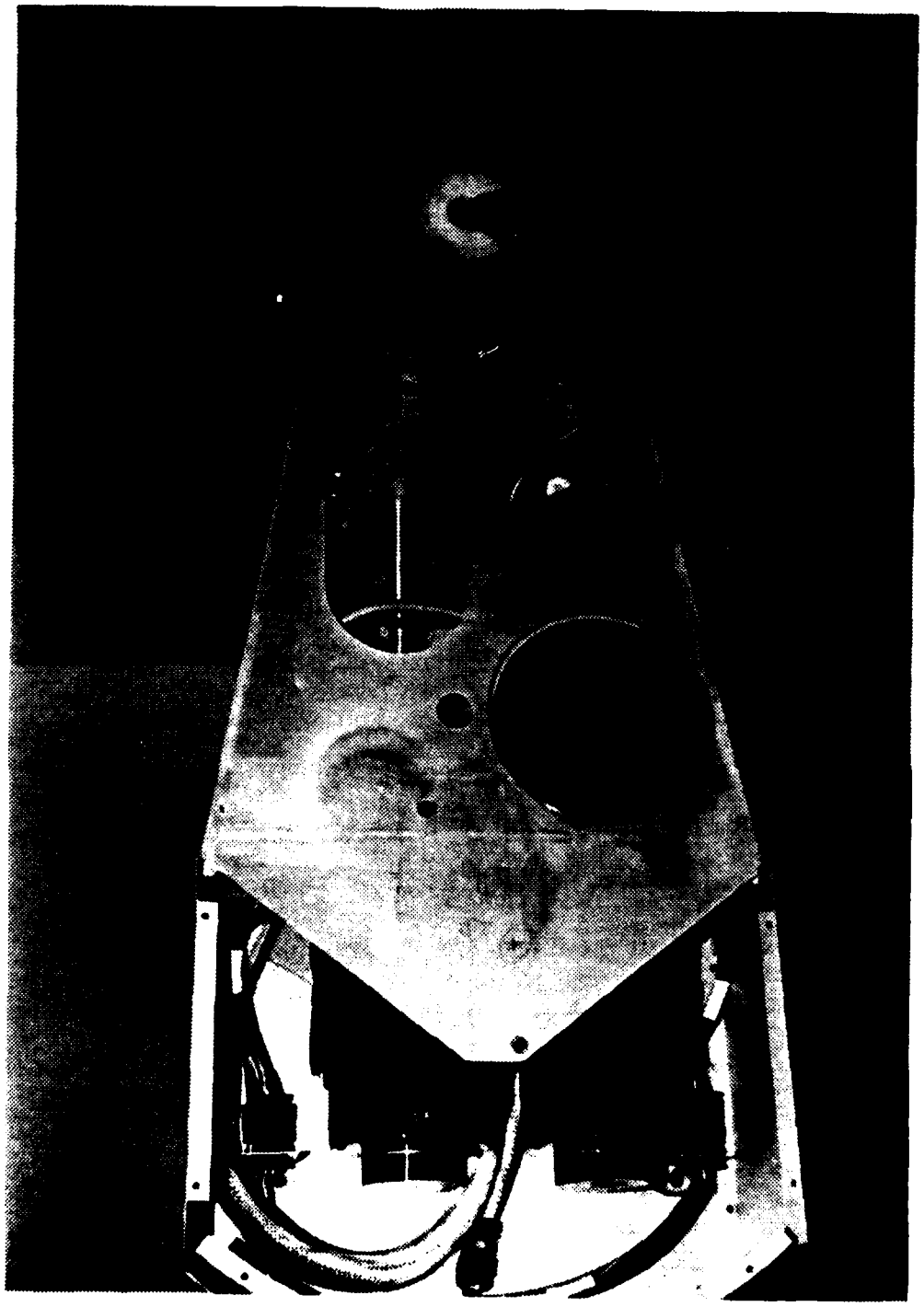

Figure 28. Shoulder Link Drive Train

AT expansion slots. Each pair of boards will sample six encoders and provide position signals to the computer through addressable ports. A total of 12 encoders will be used to gather data. Six that exist on the drive motors and six that will be added nearer to each joint. The angle due to flexibilities will be the difference between the pair of encoders at each joint.

With the robot arm joints instrumented, the dynamic response can be measured. This data will help to develop and verify the flexible model. The added encoders can also be integrated into future control schemes to provide more precise joint angle feedback.

IV. CONCLUSIONS

The following conclusions can be drawn:

1. The flexibility of each joint in the PUMA 560 robot can be modeled as a linear quantity with a torsional spring constant 'k' of:

Joint 1	68,000 N-M/RAD
Joint 2	66,500 N-M/RAD
Joint 3	11,650 N-M/RAD
Joint 4	2,150 N-M/RAD
Joint 5	1,130 N-M/RAD
Joint 6	1,680 N-M/RAD

2. The effects of gear-lash are adequately compensated for in the PUMA 560 robot and can be neglected in the development of the flexible model. The special case for joint one may require a torque limit in the final controller design.
3. This detailed examination of the PUMA 560 robot arm and its drive train flexibilities has shown that there is potential to compensate for joint flexibility. This will allow an increase in performance of 50 to 75% with the current mechanical systems.

V. RECOMMENDATIONS

The following are recommendations for further research:

1. Instrument the PUMA 560 robot joints to provide the actual joint angle.
2. Develop the equations of motion to include the joint flexibilities and verify them using the instrumented arm.
3. With the model based on the joint flexibilities, develop control schemes to adequately control the arm at enhanced payloads and speeds.

LIST OF REFERENCES

1. Ahamad S., "Second Order Nonlinear Kinematic Effects, and Their Compensation," IEEE INTERNATIONAL CONFERENCE ON Robotics and Automation Proceedings, pp. 310-317, St.Louis, MO, March 1985.

2. Good M.C., Sweet L.M., Strobel,K.L., "Dynamic Models for Control System Design of Integrated Robot and Drive Systems," Journal of Dynamic Systems, Measurement, and Control, Vol 107, pp. 53-59, March 1985.

3. Unimation, A Westinghouse Company, Unimate PUMA Mark II Robot, 500 Series Equipement Manual, 398AG1, August 1985.

4. Unimation, A Westinghouse Company, Unimate Industrial Robot Programming Manual, Users Guide to VAL II Version 2.0, 398U1, February 1986.

5. Snyder, W.E., Industrial Robots, Computer Interfacing and Control, pp. 24-38, Prentice-Hall, Inc., 1985.

TABLE 1 - JOINT ONE EXPERIMENTAL DATA

TORQUE N-M	CCW-1 RAD	CW-1 RAD	CCW-2 RAD	CW-2 RAD	CCW-3 RAD	CW-3 RAD
118.713	5.480E-3	5.480E-3	5.480E-3	5.480E-3	5.480E-3	5.480E-3
101.754	5.226E-3	5.311E-3	5.198E-3	5.311E-3	5.254E-3	5.311E-3
84.795	4.972E-3	5.085E-3	4.972E-3	5.085E-3	4.972E-3	5.085E-3
67.836	4.633E-3	4.802E-3	4.633E-3	4.802E-3	4.633E-3	4.802E-3
50.877	3.107E-3	3.277E-3	3.249E-3	3.390E-3	3.164E-3	3.333E-3
33.918	2.203E-3	2.486E-3	2.232E-3	2.486E-3	2.260E-3	2.486E-3
27.134	2.090E-3	2.373E-3	2.090E-3	2.373E-3	2.119E-3	2.373E-3
20.351	1.977E-3	2.260E-3	1.977E-3	2.260E-3	1.977E-3	2.260E-3
13.567	1.864E-3	2.147E-3	1.864E-3	2.147E-3	1.864E-3	2.147E-3
6.784	1.751E-3	2.006E-3	1.780E-3	2.034E-3	1.808E-3	2.034E-3
0.000	1.638E-3	1.864E-3	1.638E-3	1.921E-3	1.638E-3	1.864E-3
-6.784	1.525E-3	1.864E-3	1.525E-3	1.808E-3	1.525E-3	1.808E-3
-13.567	1.356E-3	1.751E-3	1.384E-3	1.723E-3	1.412E-3	1.638E-3
-20.351	1.243E-3	1.638E-3	1.271E-3	1.582E-3	1.328E-3	1.582E-3
-27.134	1.130E-3	1.497E-3	1.215E-3	1.497E-3	1.243E-3	1.497E-3
-33.918	1.073E-3	1.356E-3	1.130E-3	1.356E-3	1.130E-3	1.356E-3
-50.877	8.475E-4	1.130E-3	9.040E-4	1.130E-3	9.040E-4	1.130E-3
-67.836	6.215E-4	7.910E-4	6.780E-4	8.757E-4	6.780E-4	8.757E-4
-84.795	4.237E-4	5.932E-4	4.802E-4	6.215E-4	4.520E-4	5.650E-4
-101.754	2.260E-4	3.672E-4	2.825E-4	3.955E-4	2.825E-4	3.955E-4
-118.713	0.000	1.695E-4	1.695E-4	1.695E-4	1.695E-4	1.130E-4

TABLE 2 - JOINT TWO EXPERIMENTAL DATA

TORQUE N-M	UP-1 RAD	DOWN-1 RAD	UP-2 RAD	DOWN-2 RAD	UP-3 RAD	DOWN-3 RAD
69.994	2.051E-3	2.051E-3	2.051E-3	2.051E-3	2.051E-3	2.051E-3
59.995	1.795E-3	1.949E-3	1.846E-3	1.949E-3	1.846E-3	1.949E-3
49.996	1.590E-3	1.744E-3	1.590E-3	1.769E-3	1.590E-3	1.795E-3
39.997	1.333E-3	1.487E-3	1.385E-3	1.487E-3	1.385E-3	1.487E-3
29.997	1.179E-3	1.282E-3	1.205E-3	1.282E-3	1.205E-3	1.282E-3
19.998	1.026E-3	1.128E-3	1.026E-3	1.128E-3	1.026E-3	1.128E-3
15.999	9.487E-4	1.077E-3	9.744E-4	1.077E-3	9.744E-4	1.077E-3
11.999	8.718E-4	1.026E-3	9.231E-4	1.026E-3	9.231E-4	1.026E-3
7.999	8.205E-4	9.744E-4	8.718E-4	9.744E-4	8.718E-4	9.744E-4
4.000	7.692E-4	8.974E-4	8.205E-4	9.231E-4	8.205E-4	9.231E-4
0.000	7.179E-4	8.205E-4	7.692E-4	8.462E-4	7.436E-4	8.462E-4
-4.000	6.667E-4	7.692E-4	6.667E-4	7.692E-4	6.923E-4	7.692E-4
-7.999	6.154E-4	7.179E-4	6.410E-4	7.179E-4	6.410E-4	6.923E-4
-11.999	5.641E-4	6.667E-4	5.897E-4	6.667E-4	5.897E-4	6.667E-4
-15.999	5.128E-4	6.154E-4	5.385E-4	6.154E-4	5.385E-4	6.154E-4
-19.998	4.615E-4	5.641E-4	4.872E-4	5.641E-4	5.128E-4	5.641E-4
-29.997	3.333E-4	4.103E-4	3.590E-4	4.359E-4	3.590E-4	4.359E-4
-39.997	2.051E-4	3.077E-4	2.564E-4	3.077E-4	2.564E-4	3.077E-4
-49.996	1.026E-4	1.538E-4	1.282E-4	1.795E-4	1.282E-4	1.538E-4
-59.995	0.000	5.128E-5	0.000	5.128E-5	2.564E-5	5.128E-5
-69.994	-5.128E-5	-5.128E-5	-5.128E-5	-5.128E-5	-5.128E-5	-5.128E-5

TABLE 3 - JOINT THREE EXPERIMENTAL DATA

TORQUE N-M	UP-1 RAD	DOWN-1 RAD	UP-2 RAD	DOWN-2 RAD	UP-3 RAD	DOWN-3 RAD
40.674	6.593E-3	6.593E-3	6.593E-3	6.593E-3	6.593E-3	6.593E-3
33.895	6.000E-3	6.296E-3	6.074E-3	6.296E-3	6.074E-3	6.296E-3
27.116	5.407E-3	5.926E-3	5.481E-3	5.926E-3	5.481E-3	5.926E-3
20.337	4.889E-3	5.407E-3	4.889E-3	5.407E-3	4.889E-3	5.407E-3
13.558	4.296E-3	4.815E-3	4.370E-3	4.889E-3	4.370E-3	4.889E-3
10.846	4.000E-3	4.667E-3	4.074E-3	4.667E-3	4.074E-3	4.667E-3
8.135	3.778E-3	4.370E-3	3.778E-3	4.370E-3	3.778E-3	4.370E-3
5.423	3.481E-3	4.074E-3	3.556E-3	4.074E-3	3.556E-3	4.074E-3
2.712	3.259E-3	3.778E-3	3.259E-3	3.778E-3	3.259E-3	3.778E-3
0.000	2.963E-3	3.481E-3	3.037E-3	3.481E-3	3.037E-3	3.481E-3
-2.712	2.741E-3	3.111E-3	2.741E-3	3.111E-3	2.741E-3	3.111E-3
-5.423	2.444E-3	2.815E-3	2.519E-3	2.889E-3	2.519E-3	2.889E-3
-8.135	2.222E-3	2.593E-3	2.296E-3	2.593E-3	2.296E-3	2.593E-3
-10.846	2.000E-3	2.370E-3	2.074E-3	2.370E-3	2.074E-3	2.370E-3
-13.558	1.852E-3	2.148E-3	1.852E-3	2.148E-3	1.852E-3	2.148E-3
-20.337	1.259E-3	1.556E-3	1.259E-3	1.556E-3	1.259E-3	1.556E-3
-27.116	7.407E-4	1.037E-3	8.148E-4	1.037E-3	8.148E-4	1.037E-3
-33.895	2.963E-4	5.185E-4	3.704E-4	5.185E-4	3.704E-4	5.185E-4
-40.674	0.000	0.000	0.000	0.000	0.000	0.000

TABLE 4 - JOINT FOUR EXPERIMENTAL DATA

TORQUE N-M	CCW-1 RAD	CW-1 RAD	CCW-2 RAD	CW-2 RAD	CCW-3 RAD	CW-3 RAD
9.550	8.682E-3	8.682E-3	8.727E-3	8.727E-3	8.727E-3	8.727E-3
7.991	8.273E-3	8.273E-3	8.364E-3	8.364E-3	8.364E-3	8.364E-3
6.432	7.909E-3	7.909E-3	7.909E-3	7.909E-3	7.955E-3	8.000E-3
5.262	7.545E-3	7.591E-3	7.591E-3	7.636E-3	7.636E-3	7.636E-3
4.093	7.182E-3	7.273E-3	7.273E-3	7.273E-3	7.273E-3	7.364E-3
2.923	6.818E-3	6.909E-3	6.864E-3	6.955E-3	6.909E-3	7.000E-3
2.339	6.591E-3	6.727E-3	6.682E-3	6.773E-3	6.727E-3	6.818E-3
1.754	6.364E-3	6.545E-3	6.455E-3	6.591E-3	6.455E-3	6.636E-3
1.169	6.136E-3	6.364E-3	6.227E-3	6.409E-3	6.273E-3	6.455E-3
0.585	5.909E-3	6.182E-3	6.000E-3	6.227E-3	6.045E-3	6.273E-3
0.000	5.636E-3	5.909E-3	5.727E-3	6.000E-3	5.727E-3	6.000E-3
-0.585	5.182E-3	5.545E-3	5.273E-3	5.636E-3	5.273E-3	5.636E-3
-1.169	4.818E-3	5.273E-3	4.909E-3	5.273E-3	4.909E-3	5.273E-3
-1.754	4.455E-3	4.909E-3	4.500E-3	4.909E-3	4.545E-3	5.000E-3
-2.339	4.091E-3	4.591E-3	4.136E-3	4.636E-3	4.182E-3	4.636E-3
-2.923	3.727E-3	4.273E-3	3.727E-3	4.273E-3	3.773E-3	4.318E-3
-4.093	2.909E-3	3.591E-3	3.000E-3	3.636E-3	3.000E-3	3.636E-3
-5.262	2.182E-3	2.818E-3	2.227E-3	2.909E-3	2.318E-3	2.909E-3
-6.432	1.545E-3	2.091E-3	1.636E-3	2.136E-3	1.636E-3	2.136E-3
-7.991	7.727E-4	1.000E-3	8.182E-4	1.091E-3	8.182E-4	1.091E-3
-9.550	0.000	1.818E-4	1.818E-4	1.818E-4	1.818E-4	2.273E-4

TABLE 5 - JOINT FIVE EXPERIMENTAL DATA

TORQUE N-M	UP-1 RAD	DOWN-1 RAD	UP-02 RAD	DOWN-2 RAD	UP-3 RAD	DOWN-3 RAD
10.122	0.017	0.017	0.017	0.017	0.017	0.017
8.470	0.015	0.016	0.015	0.016	0.015	0.016
6.817	0.014	0.015	0.014	0.015	0.014	0.015
5.578	0.013	0.014	0.013	0.014	0.013	0.014
4.338	0.012	0.013	0.012	0.013	0.012	0.013
3.099	0.011	0.012	0.011	0.012	0.011	0.012
2.479	0.010	0.011	0.010	0.011	0.010	0.011
1.859	9.778E-3	0.011	9.778E-3	0.011	9.778E-3	0.011
1.239	9.000E-3	0.010	9.111E-3	0.010	9.111E-3	0.010
0.620	8.333E-3	9.778E-3	8.444E-3	9.778E-3	8.333E-3	9.667E-3
0.000	7.667E-3	8.889E-3	7.667E-3	8.889E-3	7.667E-3	8.889E-3
-0.620	6.889E-3	8.111E-3	6.889E-3	8.111E-3	6.889E-3	8.056E-3
-1.239	6.278E-3	7.556E-3	6.333E-3	7.444E-3	6.222E-3	7.444E-3
-1.859	5.722E-3	6.889E-3	5.778E-3	6.778E-3	5.667E-3	6.833E-3
-2.479	5.222E-3	6.333E-3	5.222E-3	6.333E-3	5.111E-3	6.333E-3
-3.099	4.667E-3	5.778E-3	4.667E-3	5.722E-3	4.667E-3	5.778E-3
-4.338	3.667E-3	4.667E-3	3.667E-3	4.611E-3	3.667E-3	4.556E-3
-5.578	2.778E-3	3.556E-3	2.778E-3	3.556E-3	2.778E-3	3.500E-3
-6.817	1.889E-3	2.556E-3	1.944E-3	2.500E-3	1.944E-3	2.556E-3
-8.470	8.889E-4	1.333E-3	8.889E-4	1.111E-3	8.889E-4	1.278E-3
-10.122	0.000	0.000	0.000	0.000	0.000	0.000

TABLE 6 - JOINT SIX EXPERIMENTAL DATA

TORQUE N-M	CCW-1 RAD	CW-1 RAD	CCW-2 RAD	CW-2 RAD	CCW-3 RAD	CW-3 RAD
3.559	4.111E-3	4.111E-3	4.056E-3	4.056E-3	4.056E-3	4.056E-3
2.542	3.667E-3	3.778E-3	3.667E-3	3.722E-3	3.667E-3	3.722E-3
2.034	3.444E-3	3.611E-3	3.444E-3	3.556E-3	3.444E-3	3.556E-3
1.525	3.222E-3	3.444E-3	3.222E-3	3.333E-3	3.222E-3	3.333E-3
1.017	3.000E-3	3.222E-3	2.944E-3	3.222E-3	2.944E-3	3.167E-3
0.508	2.667E-3	3.000E-3	2.722E-3	3.000E-3	2.667E-3	3.000E-3
0.000	2.333E-3	2.833E-3	2.444E-3	2.778E-3	2.444E-3	2.778E-3
-0.508	2.000E-3	2.444E-3	2.000E-3	2.389E-3	2.000E-3	2.333E-3
-1.017	1.611E-3	2.000E-3	1.611E-3	2.000E-3	1.611E-3	1.944E-3
-1.525	1.222E-3	1.611E-3	1.222E-3	1.556E-3	1.222E-3	1.556E-3
-2.034	8.889E-4	1.222E-3	8.889E-4	1.167E-3	8.889E-4	1.167E-3
-2.542	5.556E-4	7.778E-4	5.000E-4	7.778E-4	5.556E-4	7.222E-4
-3.559	0.000	0.000	0.000	-1.111E-4	-1.111E-4	-1.111E-4

INITIAL DISTRUBUTION LIST

		No. Copies
1.	Defense Technical Information Center Cameron Station Alexandria, Virginia 22304-6145	2
2.	Library, Code 0142 Naval Postgraduate School Monterey, California 93943-5002	2
3.	Department Chairman, Code 69 Department of Mechanical Engineering Naval Postgraduate School Monterey, California 93943-5000	1
4.	Professor Liang-Wey Chang, Code 69Ck Department of Mechanical Engineering Naval Postgraduate School Monterey, California 93943-5000	5
5.	Professor David Smith, Code 69Sm Department of Mechanical Engineering Naval Postgraduate School Monterey, California 93943-5000	1
6.	Professor Robert Nunn, Code 69Nn Department of Mechanical Engineering Naval Postgraduate School Monterey, California 93943-5000	1
7.	Unimation, A Westinghouse Company Shelter Rock Lane Danbury, Connecticut 06810 Attn: M.J. Leninger	1

8. CDR Dave Southworth 1
ONT 227
800 N. Quincy St.
Arlington, Virginia 22217

9. Lieutenant D.K. Gonyier 2
Mare Island Naval Shipyard
Vallejo, California 94592

END

7-87

DTIC